Normal anatomy and anatomic variants of the biliary tree and pancreatic ductal system at MRCP - what the clinicians want to know

Poster No.:	C-1696
Congress:	ECR 2014
Type:	Educational Exhibit
Authors:	J. Ressurreição[1], L. Batista[1], J. T. Soares[1], I. Marques[2], E. Matos[1], L. Andrade[3], A. Almeida[1], P. Madaleno Ferreira Alves[1], P. Portugal[1]; [1]Vila Nova de Gaia/PT, [2]Vila Nova de Gaia, Porto/PT, [3]Coimbra/PT
Keywords:	Normal variants, Diagnostic procedure, Cholangiography, MR, Pancreas, Biliary Tract / Gallbladder, Anatomy, Education and training
DOI:	10.1594/ecr2014/C-1696

Learning objectives

- To describe the MRCP (magnetic resonance cholangiopancreatography) technique used in our department
- To review and illustrate the MR features of normal biliary and pancreatic ductal anatomy and the possible anatomical variants that may occur

Background

MRCP is a recent and always evolving imaging technique that has revolutionized pancreatobiliary tract evaluation, allowing it to be non-invasive, ionizing radiation-free and without the need of anesthesia. It has replaced endoscopic retrograde cholangiopancreatography (ERCP) as the modality of choice to study the pancreatobiliary tract. Unlike this invasive procedure, MRCP can be performed in patients with previous biliary surgery, namely biliary-enteric anastomosis and, as it is a non-invasive technique, it avoids some relatively common and potentially severe complications of ERCP like pancreatitis, hemorrhage, bowel perforation or infection.

One of the most important goals of MRCP is to define the biliary and pancreatic ductal anatomy. There are a large number of possible variants that can affect the biliary and pancreatic ducts, which are not generally relevant as they are not usually pathological *per se*, but that can be of ultimate importance in specific situations like hepatobiliary or gallbladder interventional procedures (surgical and non-surgical).

Findings and procedure details

- **MRCP protocol**

In our department, all patients must fast for 6 hours prior to the examination to reduce fluid secretions within the stomach and duodenum, reduce bowel peristalsis and promote gallbladder distention.

MRCP procedures are done in a *RM Siemens*® *Simphony TIM* 1.5 T and we always combine the MRCP sequences with conventional abdominal MRI imaging to evaluate extraductal structures. This includes T2-weighted half-Fourier acquisition single-shot turbo spin-echo (HASTE) in three planes, axial breath-hold T2-weighted turbo spin-echo (TSE) with fat-suppression, diffusion-weighted imaging (DWI) using single-shot

spin-echo echo-planar imaging with spectral presaturation attenuated inversion recovery (SPAIR) fat-suppressed pulse sequence with four b-values (50, 150, 500, 1000), axial dual-echo single breath-hold *in* and *opposed* phase T1-weighted images, axial fat-suppressed gradient-echo T1-weighted images using a 3D volumetric breath-hold examination (VIBE) sequence and, at last, the MRCP acquisition consisting in coronal oblique and axial 3D respiratory-triggered heavily T2-weighted fast spin echo (FSE) sequences (MRCP imaging parameters in Table 1 on page 7). The whole study usually lasts around 18 to 20 minutes in a cooperative, non-ascites patient. Maximum intensity projection (MIP) reformats can be generated from MRCP sequences, allowing to obtain multiplanar images with different slice thickness.

If there is a suspicion of any ductal wall or parenchymal focal lesion, dynamic gadolinium-enhanced axial fat-suppressed gradient-echo T1-weighted VIBE sequences are acquired.

- **Normal biliary ductal anatomy (Fig. 1 on page 8, Fig. 2 on page 9, Fig. 3 on page 10, Fig. 4 on page 11)**

The biliary drainage system consists of several ducts that run parallel to the portal venous supply to drain the different hepatic segments.

The **right hepatic duct** drains the four segments of the right liver lobe which are separated by a coronal plane containing the right hepatic vein into anterior (V and VIII) and posterior (VI and VII) segments and by the right portal vein into superior (VII and VIII) and inferior (V and VI) segments. This duct divides into two main branches:

1. **Right anterior duct**, which runs vertically and drains the anterior segments;
2. **Right posterior duct**, which has a horizontal course and is responsible to drain the posterior segments.

The right posterior duct tends to course posteriorly to the right anterior duct and joins it in the medial (left) aspect to originate the usually short right hepatic duct.

The **left hepatic duct** is divided in several branches responsible for draining the four left segments of the liver. These segments are divided into lateral (II and III) and medial segments (IVa and IVb) by the umbilical fissure and falciform ligament or the left hepatic vein. The caudate lobe (segment I) is situated between the fissure for the ligamentum venosum and the inferior vena cava.

The right hepatic duct attaches to the left hepatic duct to form the **common hepatic duct**. The duct that drains the caudate lobe may join the right or the left hepatic ducts.

In the most common form, the thin and tortuous **cystic duct** measures between 2-4cm in length and usually empties into the common hepatic duct halfway between the porta hepatis and the ampulla of Vater (middle one-third), from a right lateral position, originating the **common bile duct**. It connects the gallbladder to the extrahepatic biliary tree.

- **Anatomical variants of the biliary tree**

The biliary anatomy can be very complex and there are several anatomical variants, some of them common and other less frequent. These variants generally do not have clinical significance but can increase the probability of an iatrogenic injury due to inadvertent ligation or transection during interventional procedures.

The variants that may affect the **intra-hepatic ducts** are the following:

1. **Right posterior duct draining into the left hepatic duct** (Fig. 5 on page 12 Fig. 6 on page 13). This is the most frequent anatomical variant of the biliary tree;
2. **Right posterior duct joining with the right anterior duct by its lateral (right) side** (Fig. 7 on page 14, Fig. 8 on page 15);
3. **Triple confluence**, with the right posterior, right anterior and left hepatic ducts joining at the same point to form the common hepatic duct (Fig. 9 on page 16, Fig. 10 on page 17);
4. **Right posterior duct draining directly into the common hepatic or cystic duct** (Fig. 11 on page 18, Fig. 12 on page 19).

Knowing biliary ductal anatomy with precision is very important in some procedures like the selection of donors in liver transplantation. As examples, the existence of "triple confluence" is a contraindication for safe right hepatectomy and the "right posterior duct draining into the left hepatic duct" is a contraindication for both right and left hepatectomy.

The **cystic duct** can also present anatomical variants:

1. **Low cystic duct insertion** (Fig. 13 on page 20, Fig. 14 on page 21), with the cystic duct joining the common hepatic duct at its distal third, near the ampulla of Vater;

2. **Medial cystic duct insertion** (Fig. 14 on page 21, Fig. 15 on page 22), with the cystic duct joining the common hepatic duct at its medial (left) aspect;
3. **Parallel course between the cystic duct and the common hepatic duct** (Fig. 16 on page 23, Fig. 17 on page 24), implying that the two run together for at least 2cm. It is usually associated to the presence of a common sheath around the cystic duct and the common hepatic duct;
4. **High cystic duct insertion**, with the cystic duct joining the common hepatic duct in the porta hepatis or even joining the right or left hepatic ducts (Fig. 18 on page 25, Fig. 19 on page 26).

Despite not being a routine practice (and probably not a cost-effective one), MRCP mapping of the cystic duct route can diminish the risk of complications associated to cholecystectomies, like transection of the extrahepatic bile duct. One of the anatomical variations associated to this complication is the "parallel course between the cystic duct and the common hepatic duct".

- **Normal pancreatic ductal anatomy (Fig. 20 on page 27, Fig. 21 on page 28)**

The main pancreatic duct is the canal that crosses the pancreas, from the tail to the head, with variable length and caliber. It normally has around 20-30 side branches. In the pancreatic head, the main pancreatic duct divides into the duct of Wirsung, which is posterior and drains the ventral pancreas and into the accessory duct of Santorini, which is anterior and drains the dorsal pancreas.

The duct of Wirsung, the one responsible for carrying most of the pancreatic juice, enters the duodenal wall and joins with the terminal portion of the common bile duct, draining together at the papilla major. Normally, this common channel named pancreatobiliary junction (Fig. 22 on page 29) is totally intra-mural, measuring around 10-15mm. The terminal portions of the Wirsung and common bile duct are invested together by smooth muscle fibers - the Oddi's sphincter.

The duct of Santorini terminates at the papilla minor.

- **Anatomical variants of the pancreatic ductal system**

Anatomical variants of the pancreatic ducts are generally devoid of clinical significance and frequently diagnosed incidentally, particularly after the arrival of MRCP. The most common and clinically relevant anatomical variant is pancreas *divisum*, which is thought

by some to predispose to acute pancreatitis. Pancreas *divisum* results from the non-fusion of the dorsal and ventral pancreatic buds during embryogenesis. The result is that the majority of the pancreas drains through the duct of Santorini at the minor papilla.

There are two main subtypes of pancreas divisum: complete (Fig. 23 on page 30, Fig. 24 on page 31), where there is no communication between the dorsal and ventral ducts, and incomplete (Fig. 25 on page 32, Fig. 26 on page 33), corresponding to 10-15% of cases, where a minor communication between the ducts can be seen.

- **Anomalous pancreatobiliary junction (Fig. 27 on page 34, Fig. 28 on page 35)**

This congenital anomaly represents the junction of the common bile duct and pancreatic duct outside of the duodenal wall. In this situation the common channel is usually longer than 15mm. As the sphincter of Oddi does not involve the totality of the channel, reflux of pancreatic juice to the bile ducts and of bile into the pancreatic ductal system can occur. This may cause complications like choledochal cysts and pancreatitis, respectively.

Surgical treatment is indicated in this clinical situation.

Images for this section:

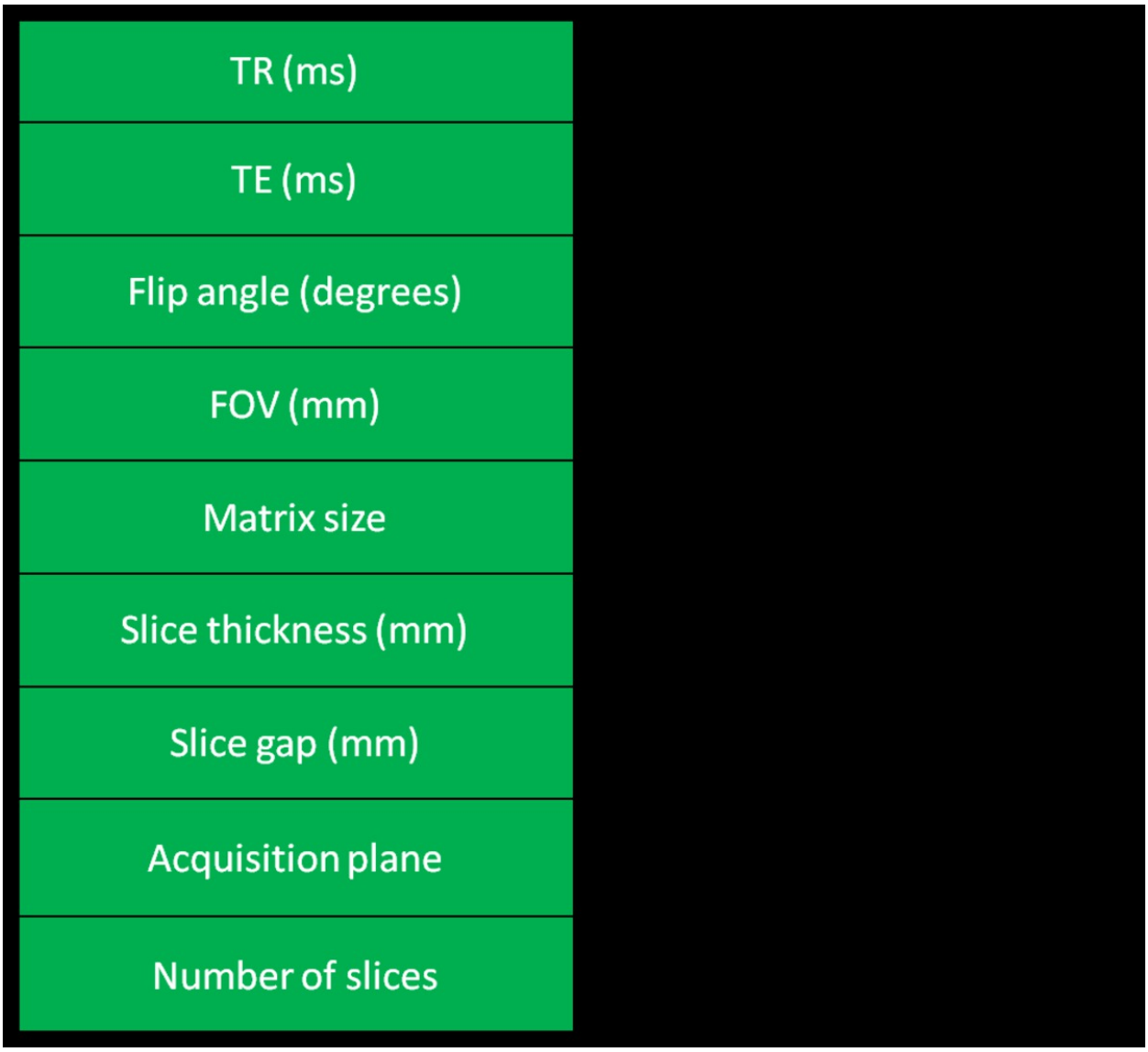

Table 1: Summary of MRCP parameters. Relaxation time (TR), echo time (TE), field of view (FOV)

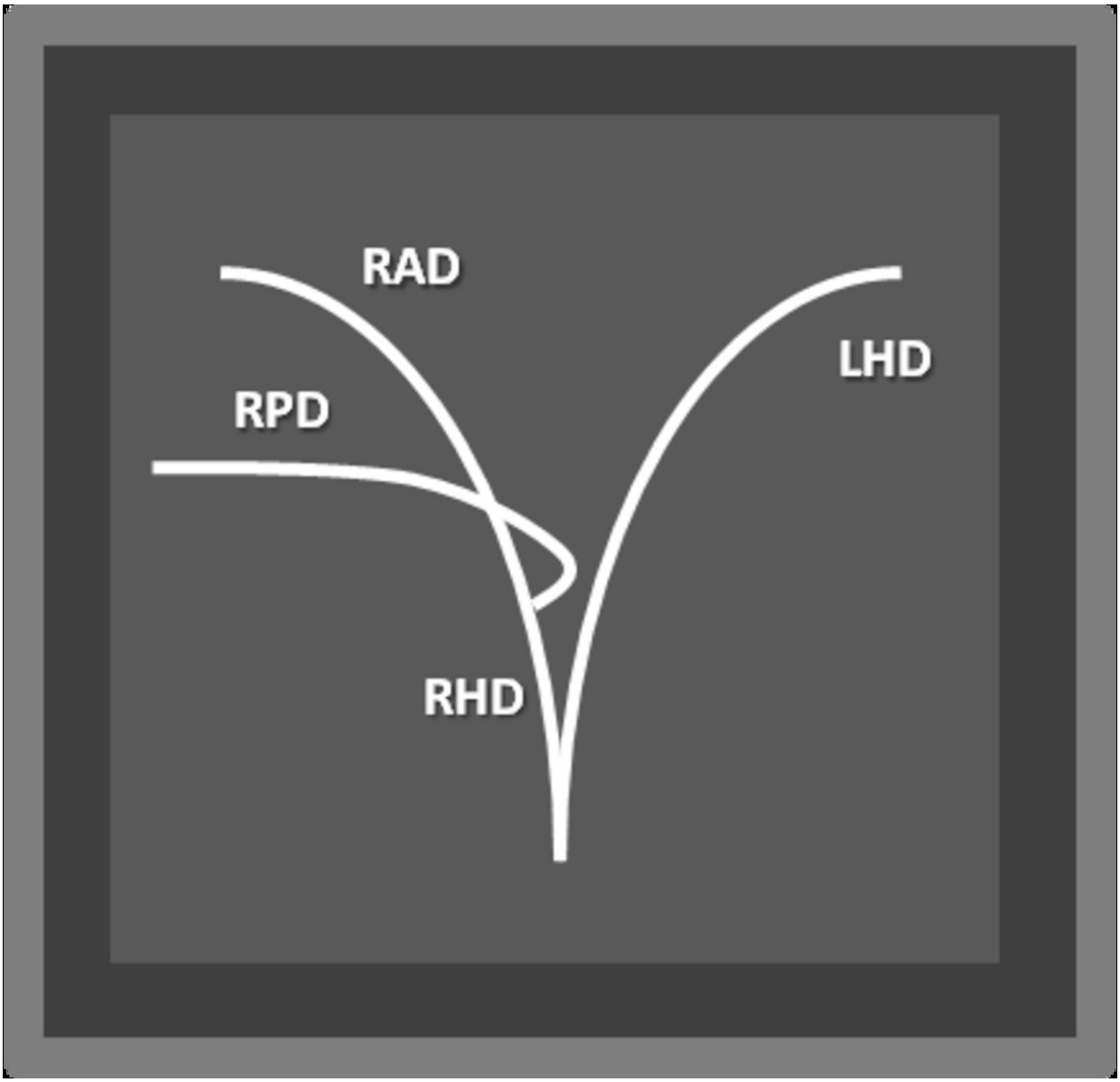

Fig. 1: "Normal hepatic ductal anatomy". Schematic representation demonstrates the confluence between the right posterior duct (RPD) and the right anterior duct (RAD), originating the right hepatic duct (RHD). Note that the RPD has a more horizontal route while the RAD is more vertical. The RHD joins the left hepatic duct (LHD).

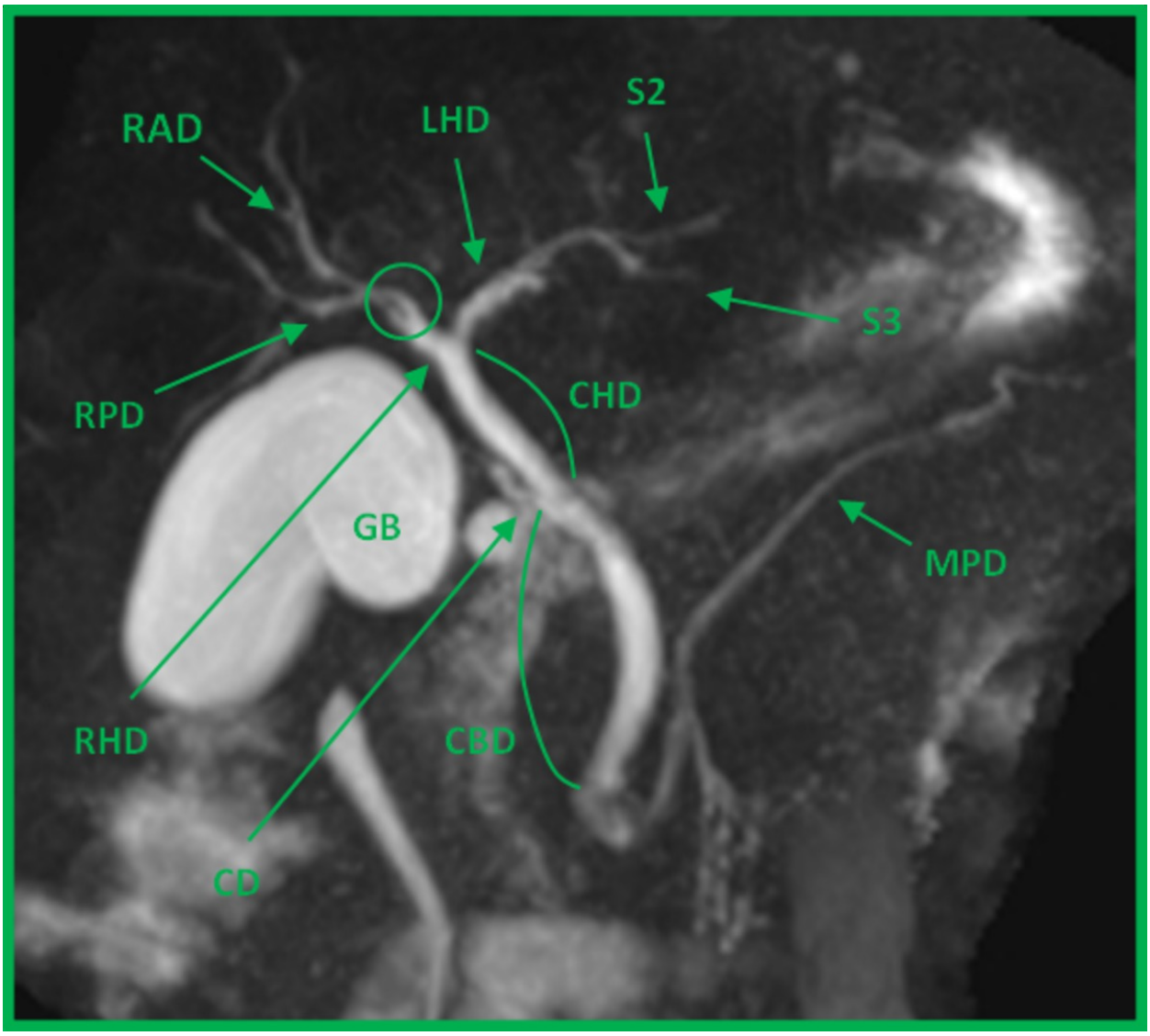

Fig. 2: "Normal hepatic ductal anatomy". Coronal oblique MIP reformat image reveals the confluence (circle) between the right posterior duct (RPD) and the right anterior duct (RAD), originating the right hepatic duct (RHD). Note that the RPD has a more horizontal route while the RAD is more vertical. By its turn the RHD joins the left hepatic duct (LHD), originating the common hepatic duct. The LHD results from the confluence of the ducts of the left hepatic lobe segments, here only represented by segments II (S2) and III (S3). Cystic duct (CD), common bile duct (CBD), main pancreatic duct (MPD), gallbladder (GB).

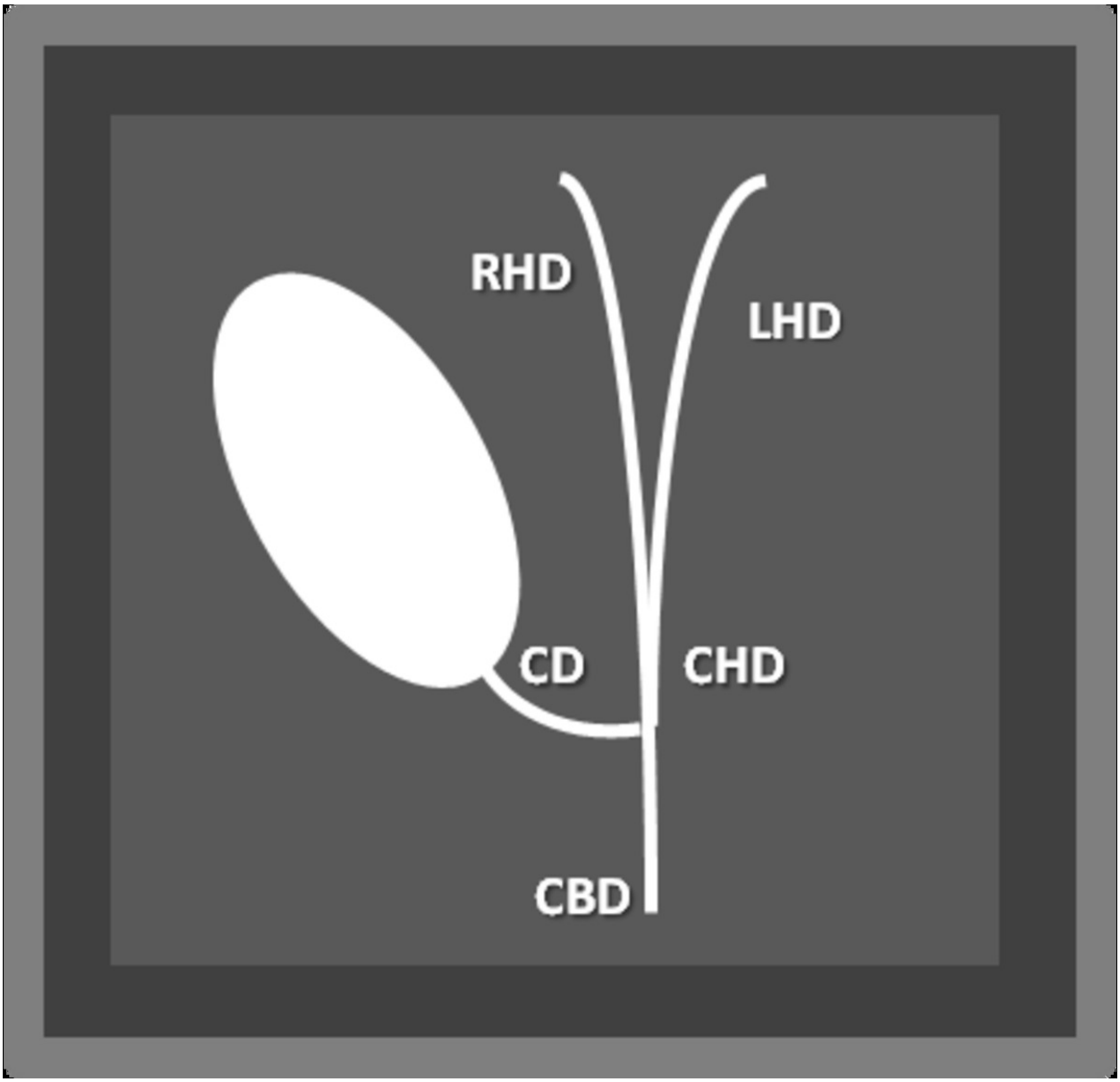

Fig. 3: "Normal extra-hepatic ductal anatomy". Schematic representation demonstrates the cystic duct (CD) emptying into the common hepatic duct (CHD), originating the common bile duct (CBD). Right hepatic duct (RHD), left hepatic duct (LHD).

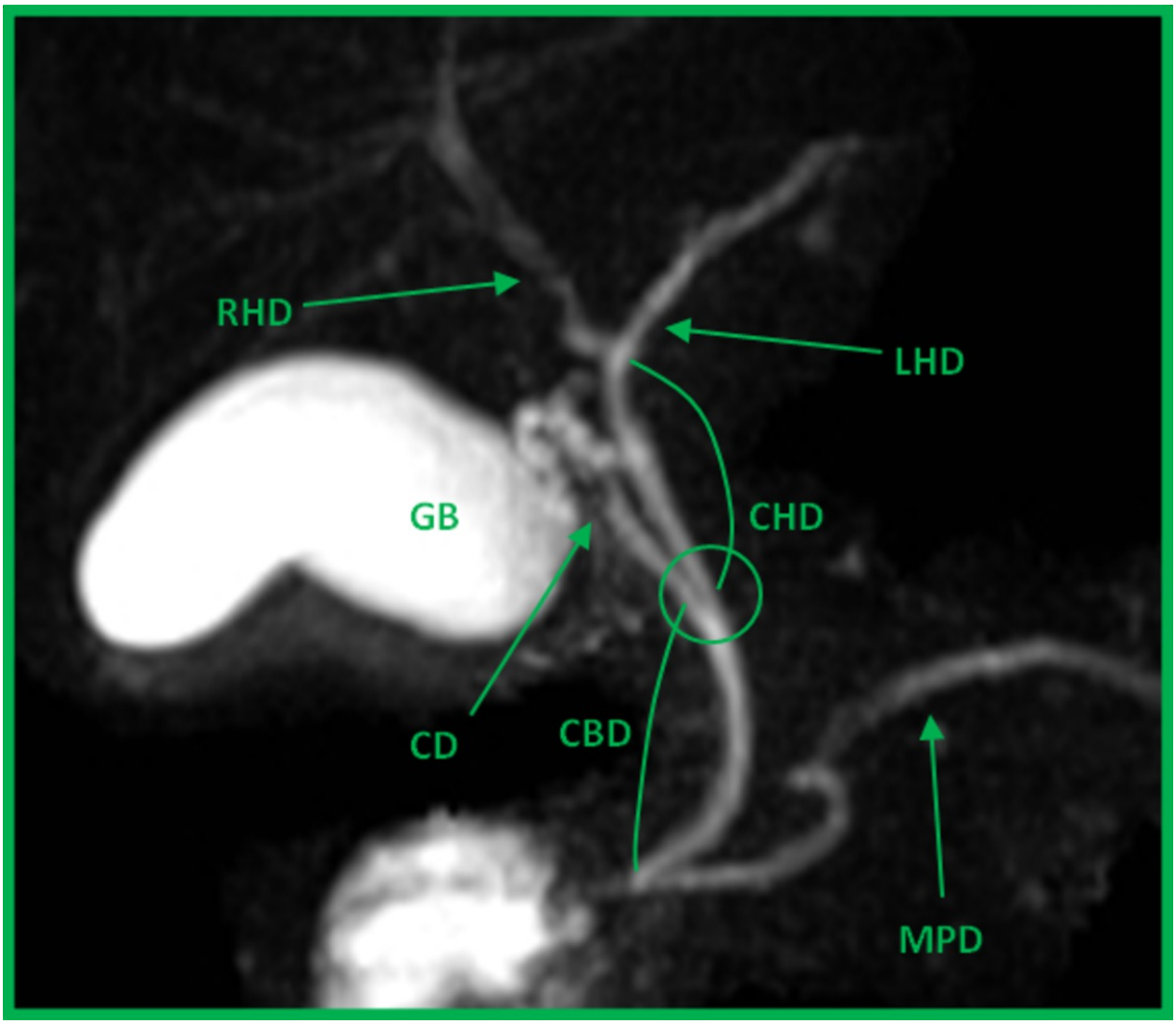

Fig. 4: "Normal extra-hepatic ductal anatomy". Coronal oblique MIP reformat image demonstrates the confluence (circle) between the partially tortuous cystic duct (CD) and the common hepatic duct (CHD), originating the common bile duct (CBD). Right hepatic duct (RHD), left hepatic duct (LHD), main pancreatic duct (MPD), gallbladder (GB).

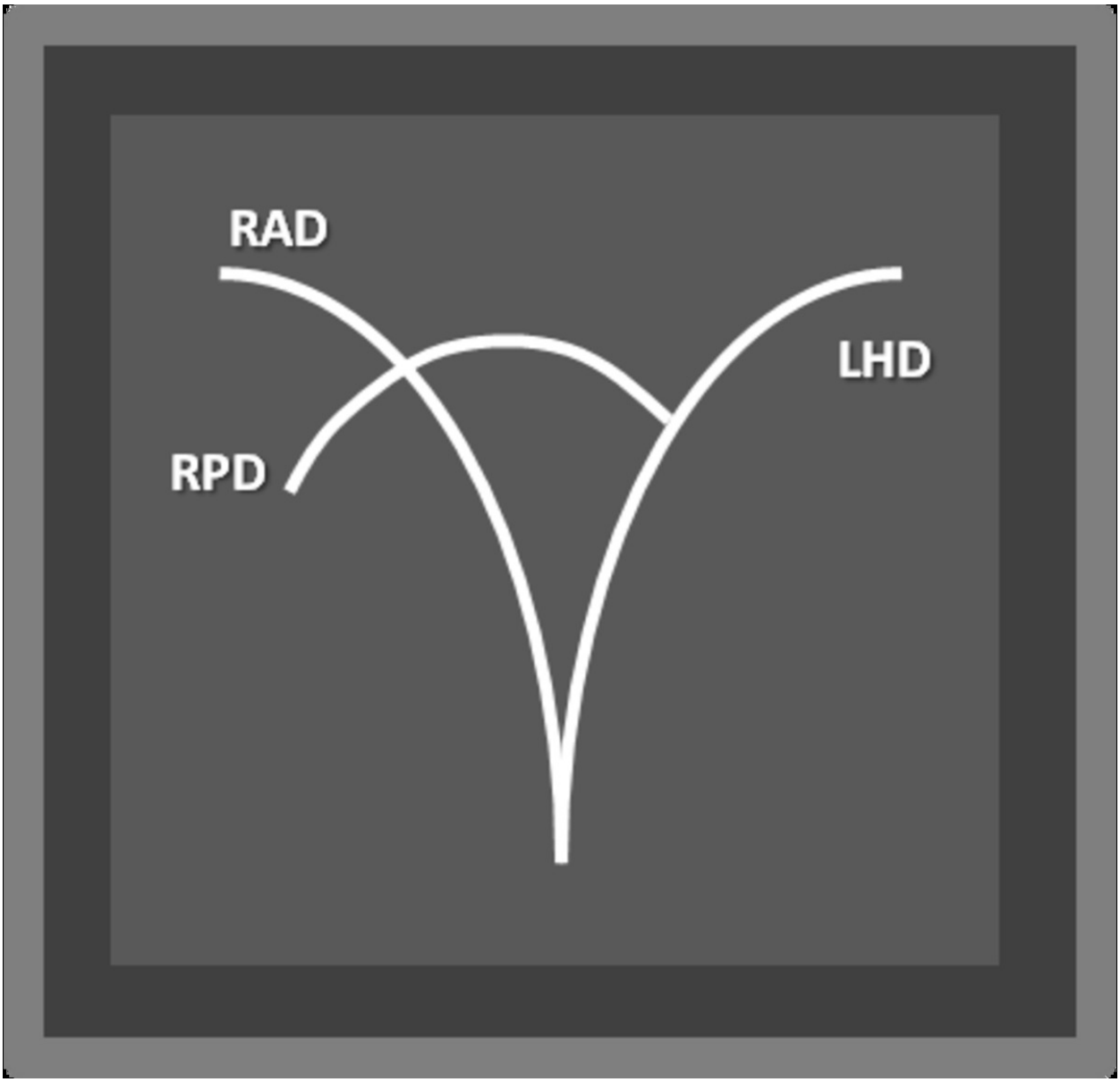

Fig. 5: "Right posterior duct draining into the left hepatic duct". Schematic representation demonstrates drainage of the right posterior duct (RPD) directly into the left hepatic duct (LHD) instead of draining into the right anterior duct (RAD).

Fig. 6: "Right posterior duct draining into the left hepatic duct". Coronal oblique MIP reformat image of a dilated biliary tree. Note that the right posterior duct (RPD) drains directly into the left hepatic duct (LHD) instead of draining into the right anterior duct (RAD). The confluence of RPD and LHD is marked by the pointing triangle.

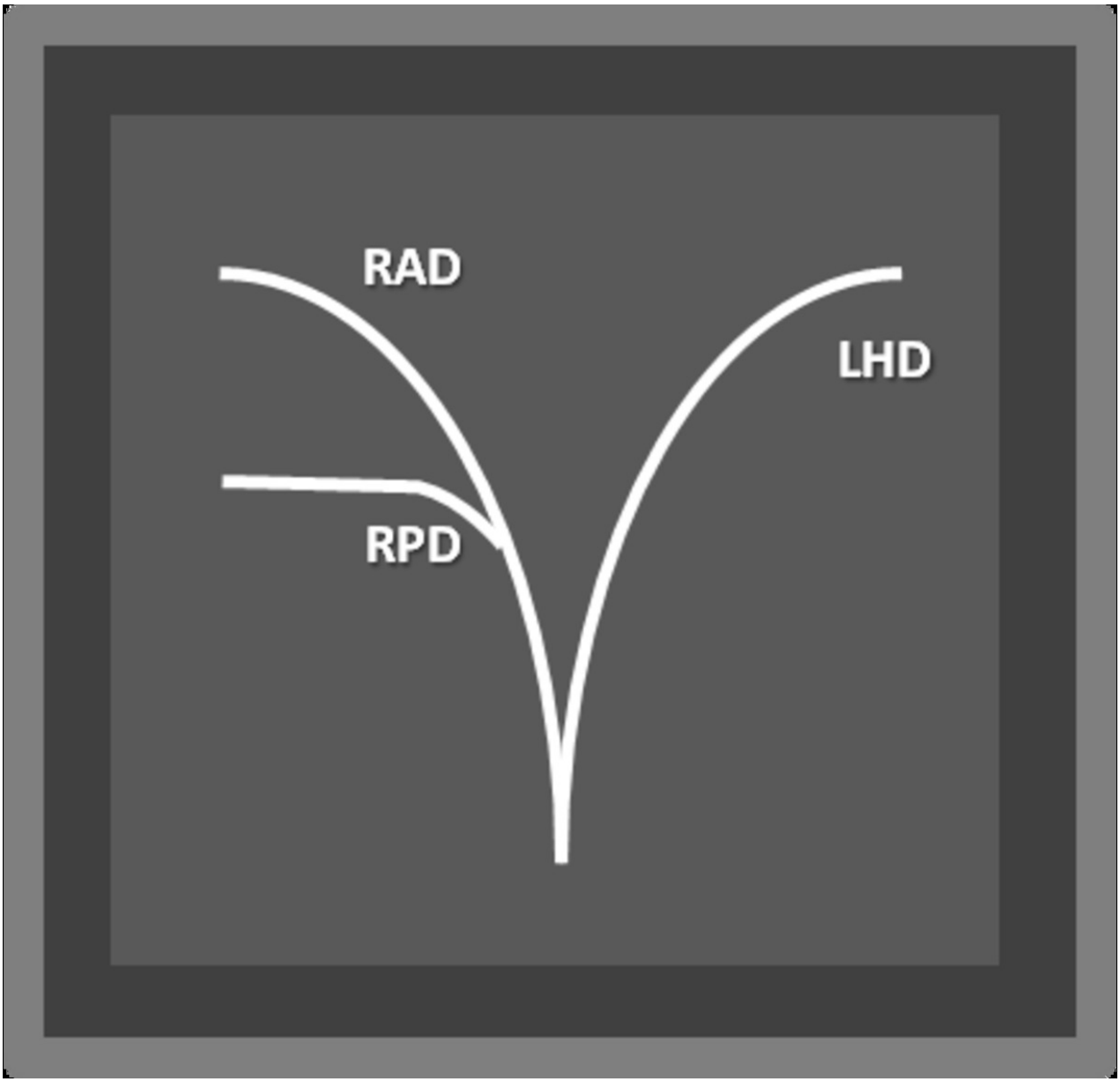

Fig. 7: "Right posterior duct joining with the right anterior duct by its lateral (right) side". Schematic representation demonstrates right-sided junction between the right posterior (RPD) and right anterior (RAD) ducts. Left hepatic duct (LHD).

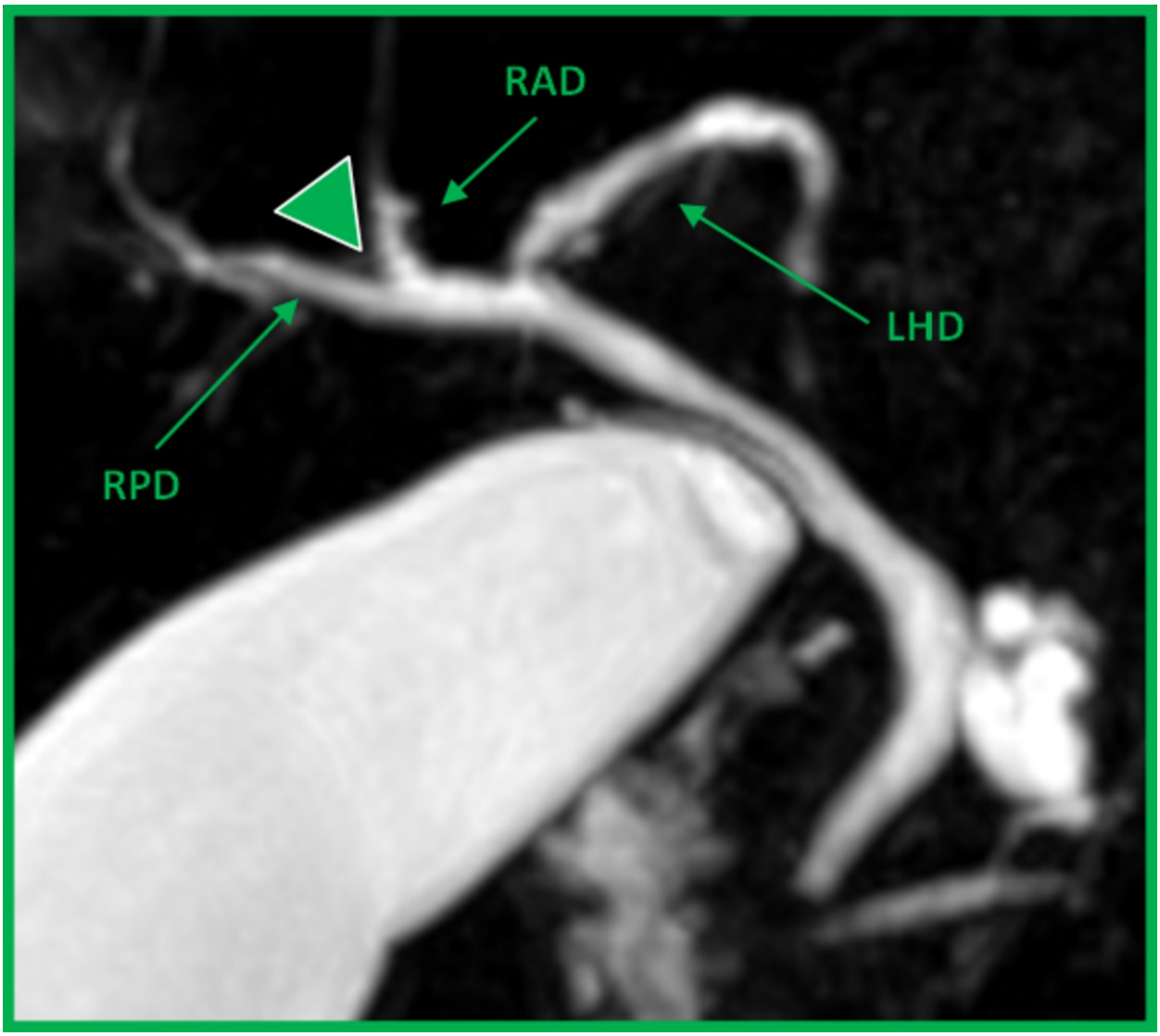

Fig. 8: "Right posterior duct joining with the right anterior duct by its lateral (right) side". Coronal oblique MIP reformat image demonstrates right-sided junction between the right posterior (RPD) and right anterior (RAD) ducts, with the confluence marked by the pointing triangle. Left hepatic duct (LHD).

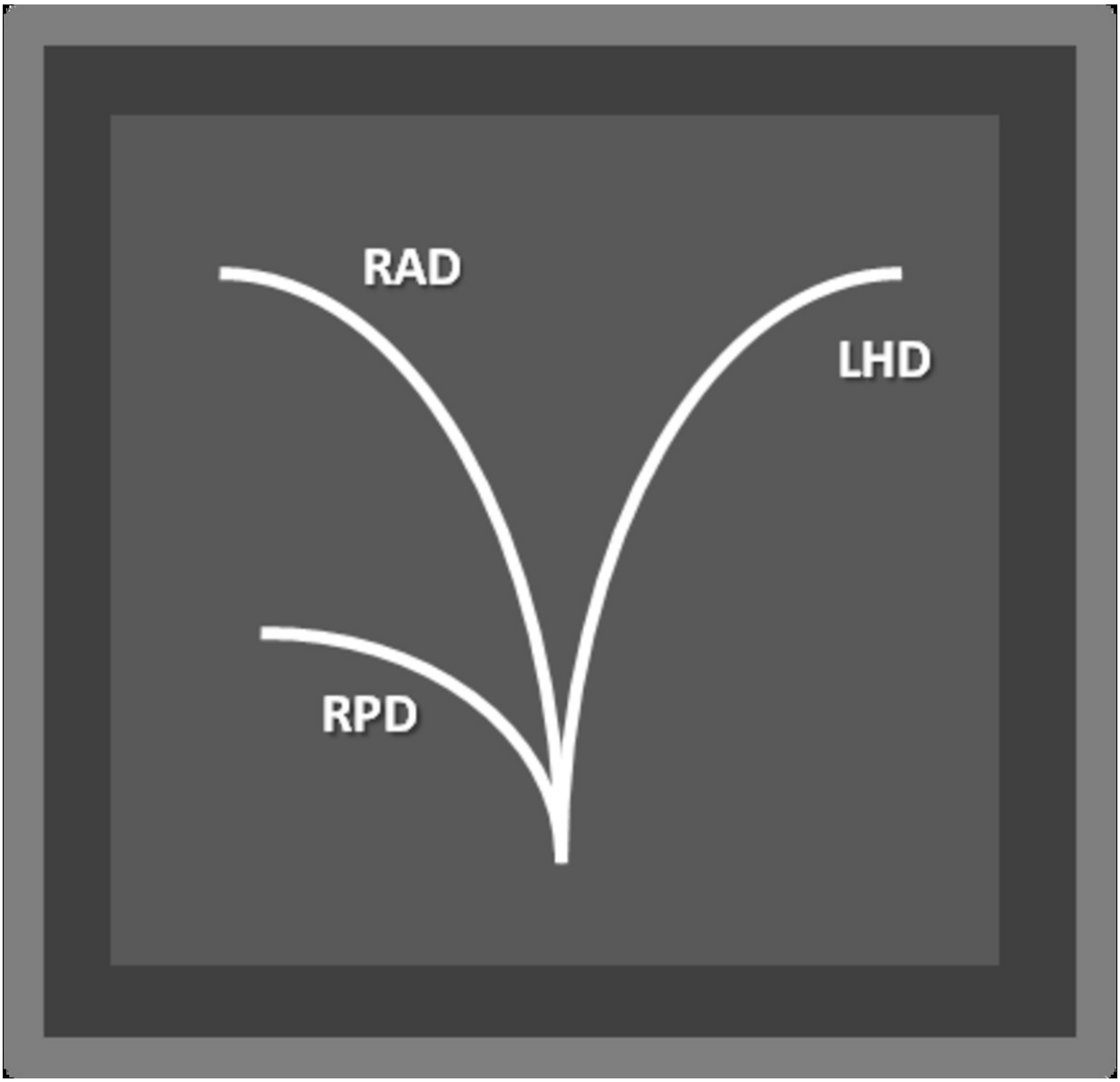

Fig. 9: "Triple confluence". Schematic representation demonstrates the common junction between the right posterior (RPD), right anterior (RAD) and left hepatic (LHD) ducts.

Fig. 10: "Triple confluence". Coronal oblique MIP reformat image reveals a common junction between the right posterior (RPD), right anterior (RAD) and left hepatic (LHD) ducts, marked by the white arrow.

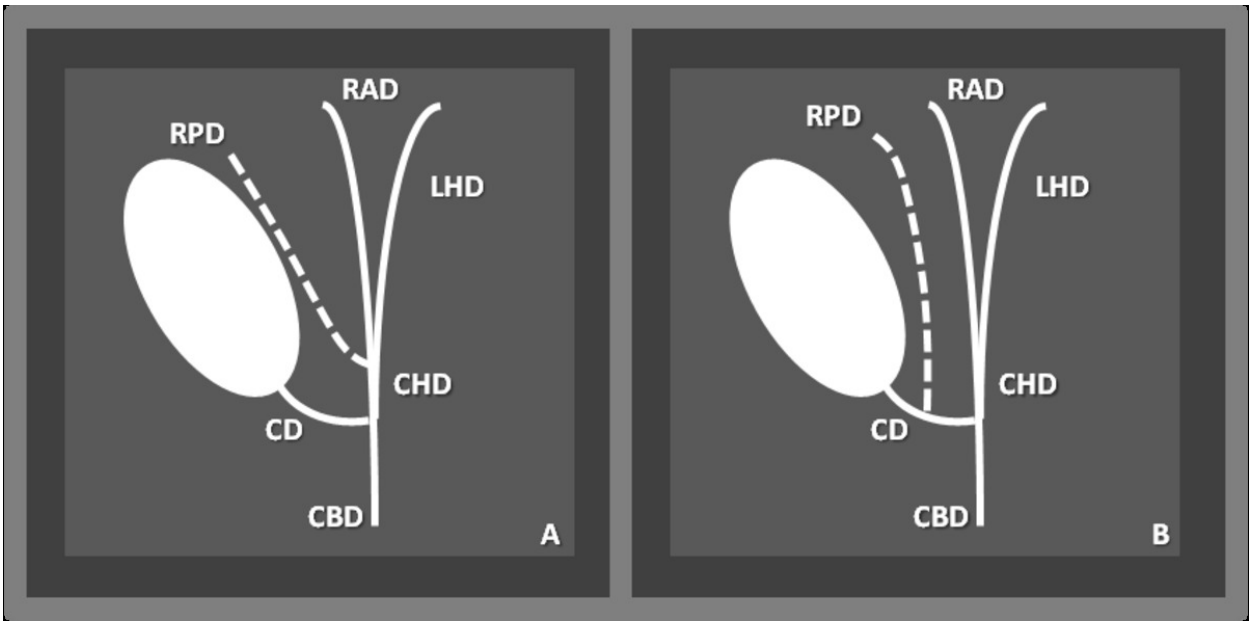

Fig. 11: (A) "Right posterior duct draining into the common hepatic duct (A) and into the cystic duct (B)". Schematic representation shows the drainage of the right posterior duct (RPD) into the common hepatic (CHD) duct (A) and into the cystic duct (B). Right anterior duct (RAD), left hepatic duct (LHD), common bile duct (CBD).

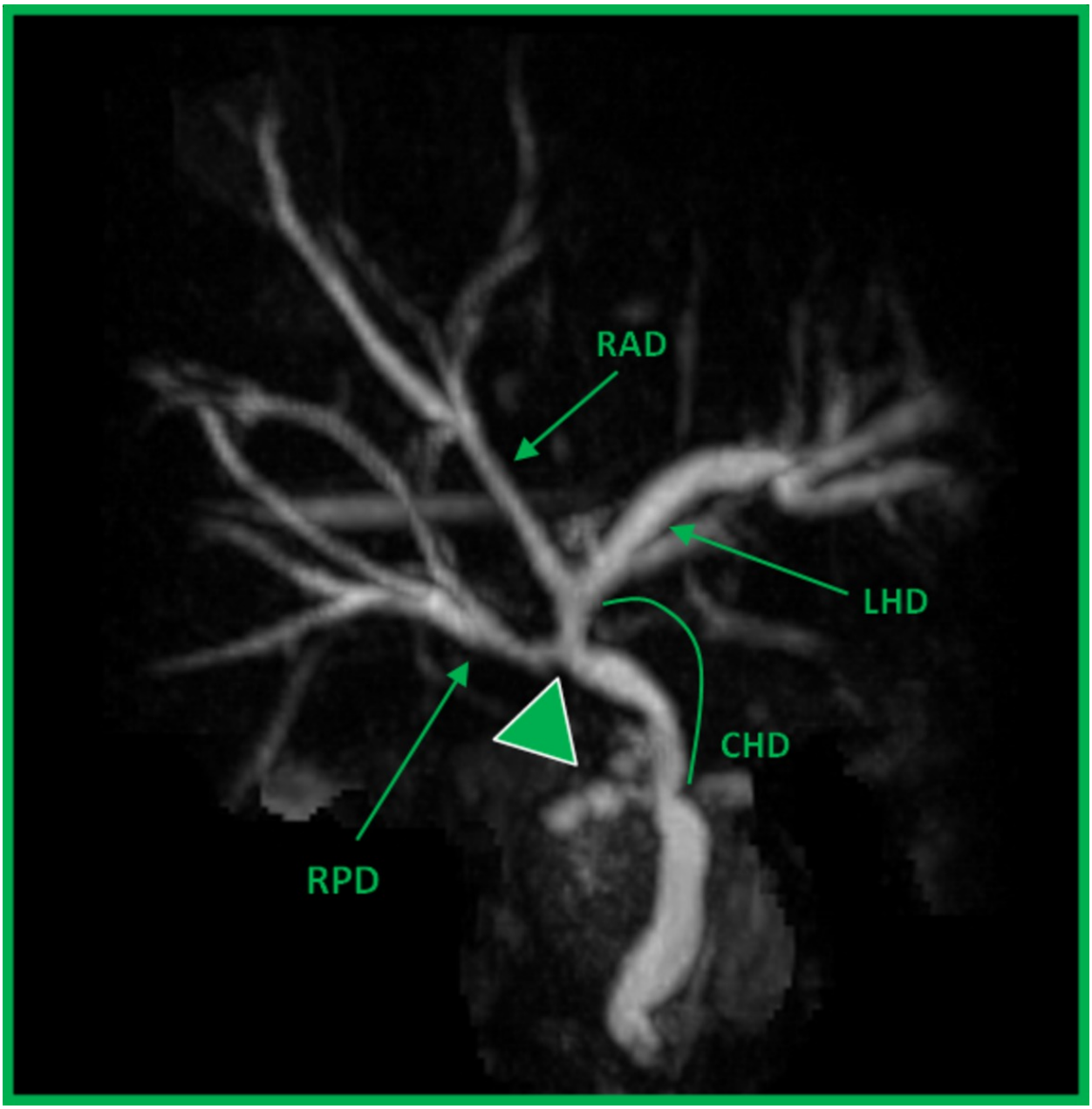

Fig. 12: "Right posterior duct draining into the common hepatic duct". Coronal oblique MIP reformat image shows the junction (pointing triangle) between the right posterior (RPD) and the common hepatic (CHD) ducts. Right anterior duct (RAD), left hepatic duct (LHD).

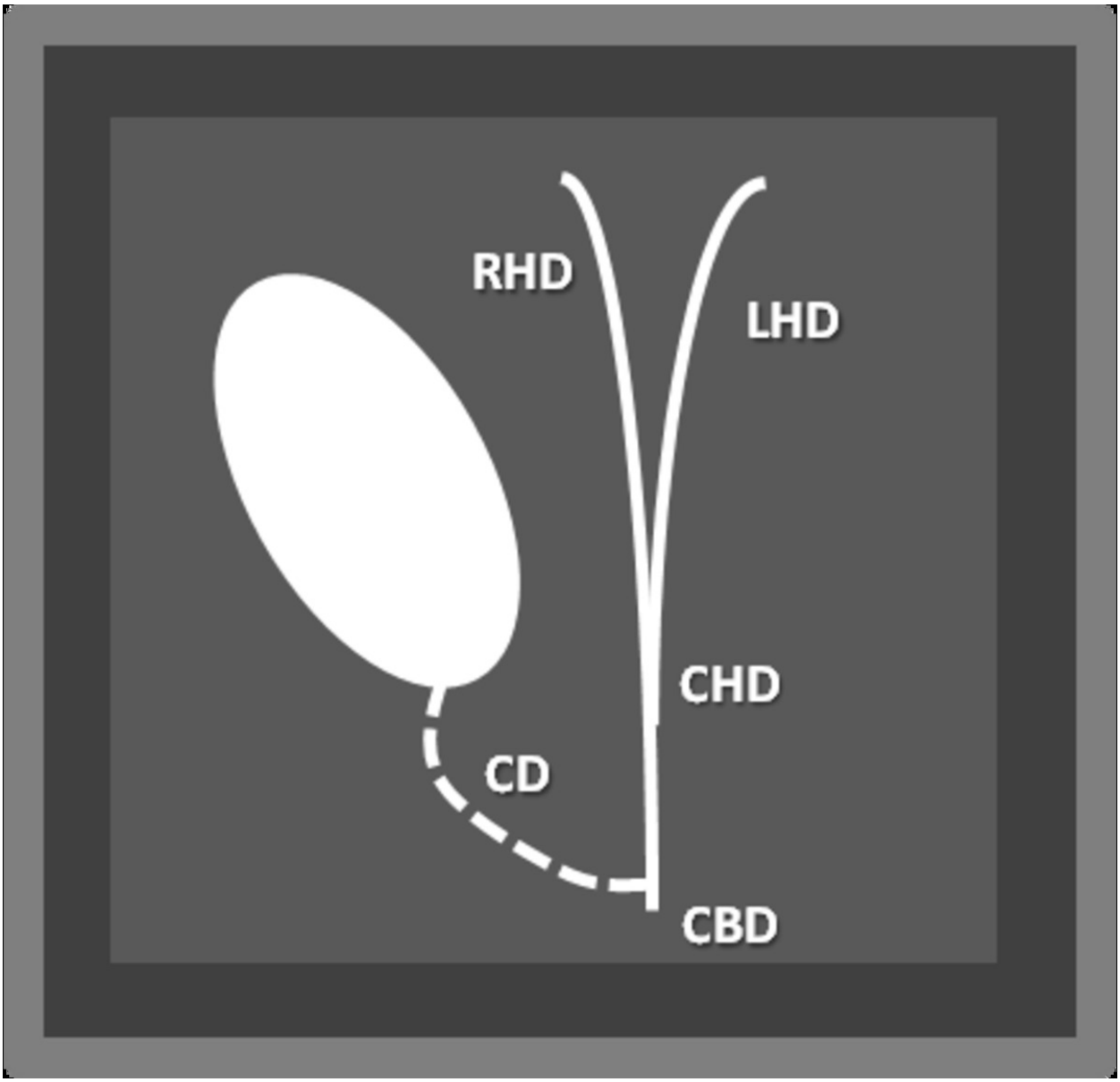

Fig. 13: "Low insertion of the cystic duct in the medial aspect of the common hepatic duct". Schematic representation demonstrates the insertion of the cystic duct (CD) in the distal third of the common hepatic duct (CHD), originating the common bile duct (CBD). Right hepatic duct (RHD), left hepatic duct (LHD).

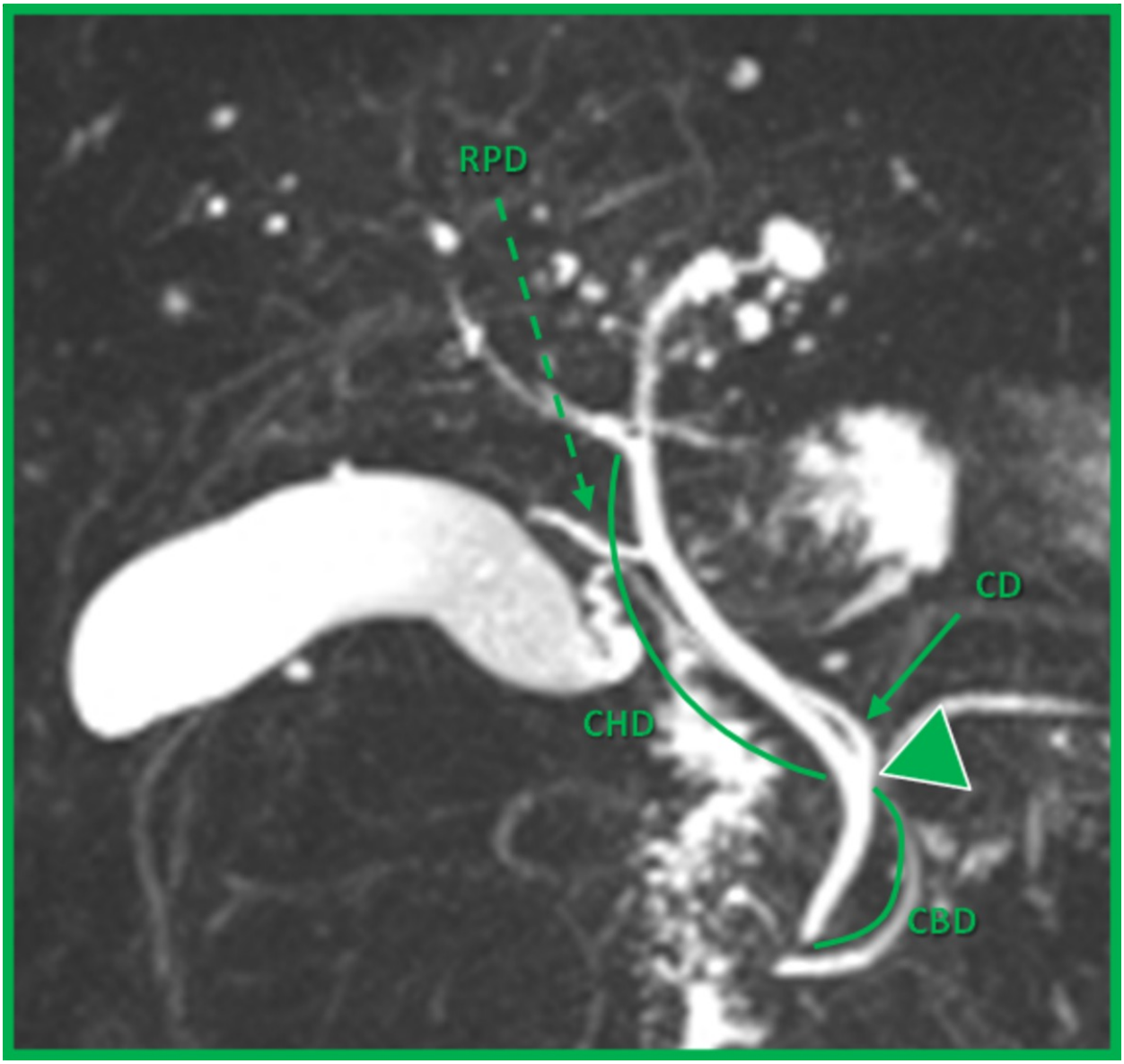

Fig. 14: "Low insertion of the cystic duct in the medial aspect of the common hepatic duct". Coronal oblique MIP reformat image demonstrates the insertion (pointing triangle) of the cystic duct (CD) in the left side of the wall of the distal third of the common hepatic duct (CHD), originating the common bile duct (CBD). It is also possible to note the junction of the right posterior duct (RPD) directly with the CHD.

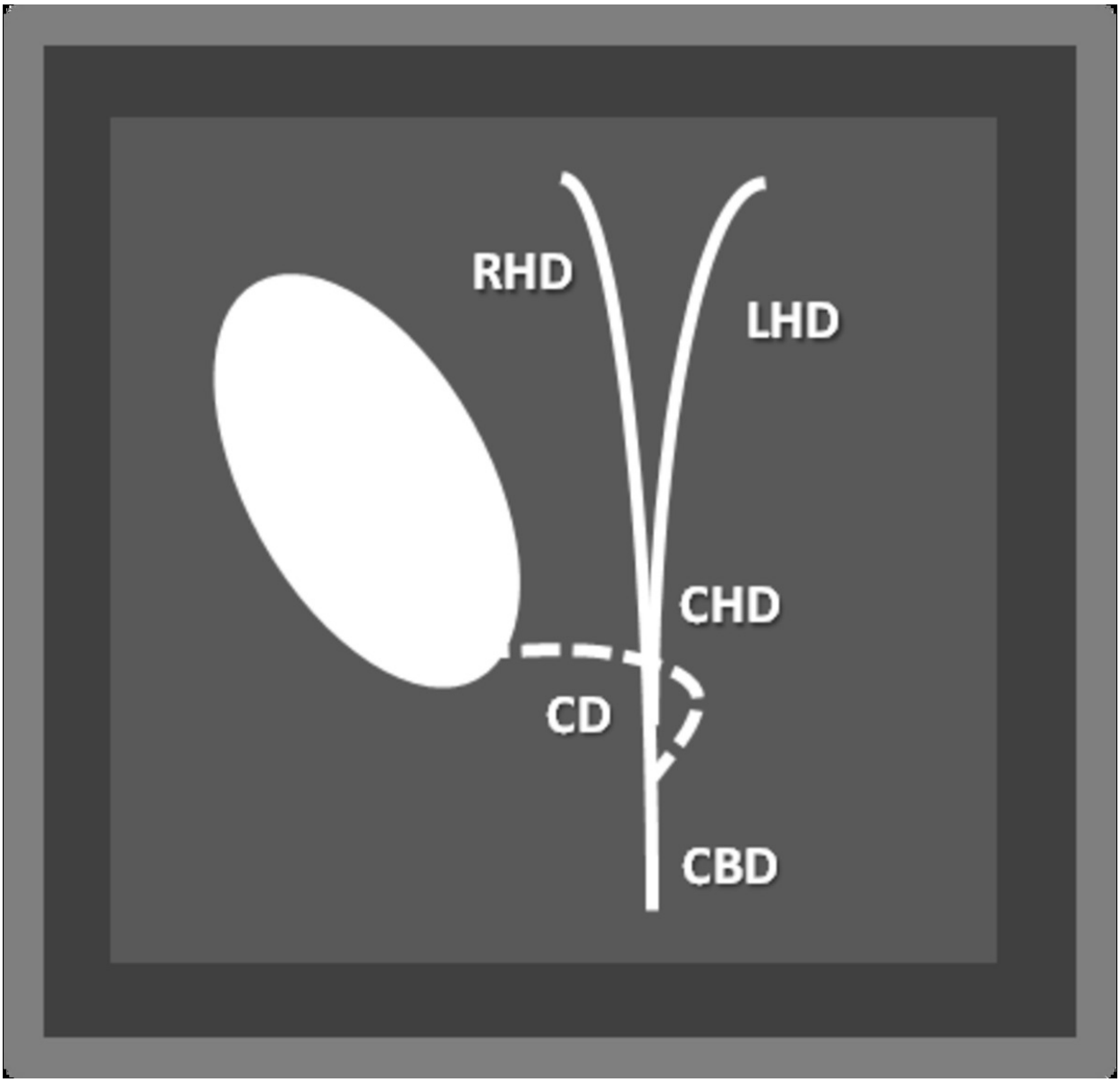

Fig. 15: "Medial insertion of the cystic duct in the medial aspect of the common hepatic duct". Schematic representation demonstrates the insertion of the cystic duct (CD) in the left side of the common hepatic duct (CHD), originating the common bile duct (CBD). Right hepatic duct (RHD), left hepatic duct (LHD).

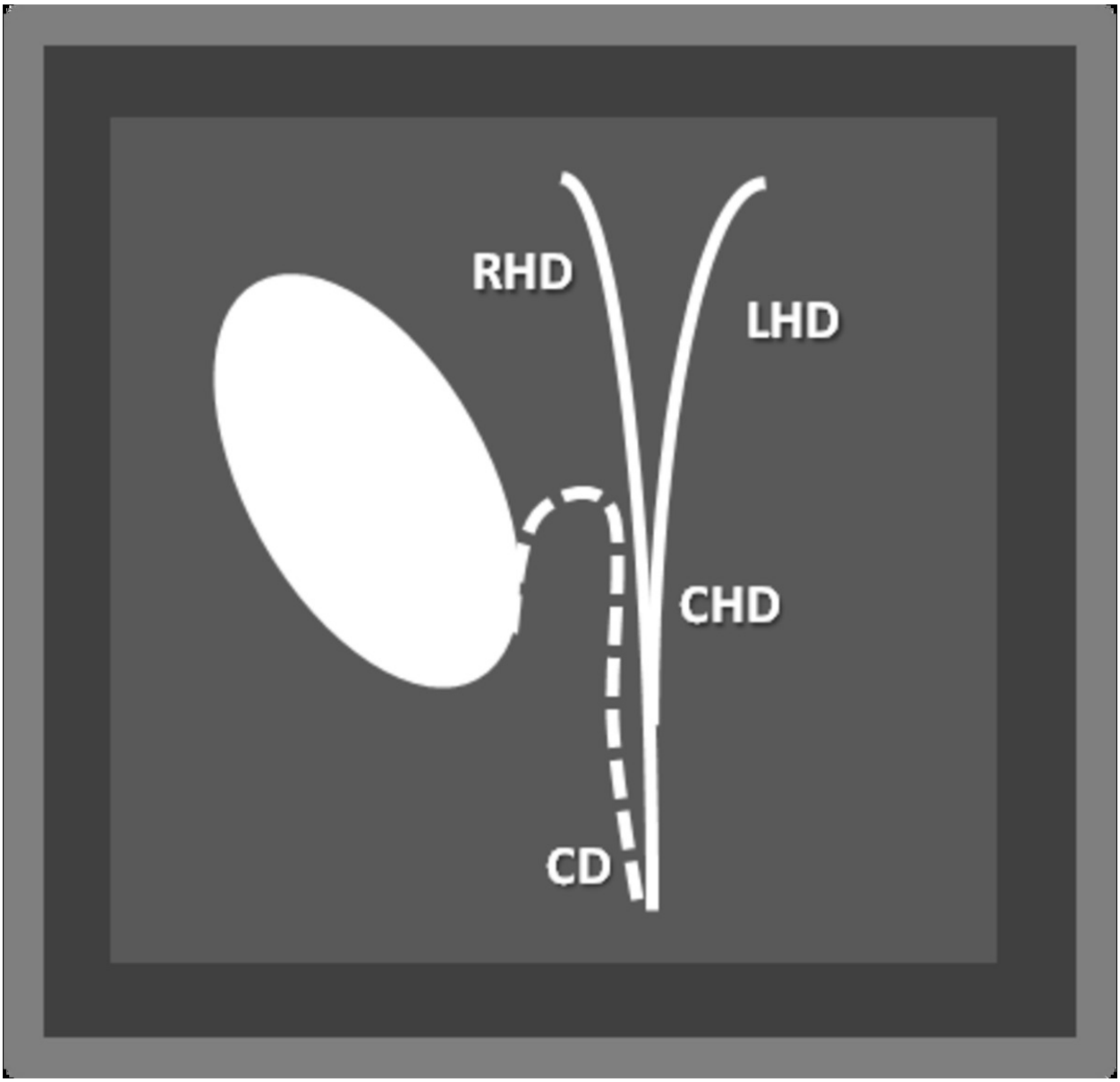

Fig. 16: "Parallel course between the cystic duct and the common hepatic duct". Schematic representation demonstrates the parallel route between long segments of the cystic (CD) and common hepatic (CHD) ducts. Right hepatic duct (RHD), left hepatic duct (LHD).

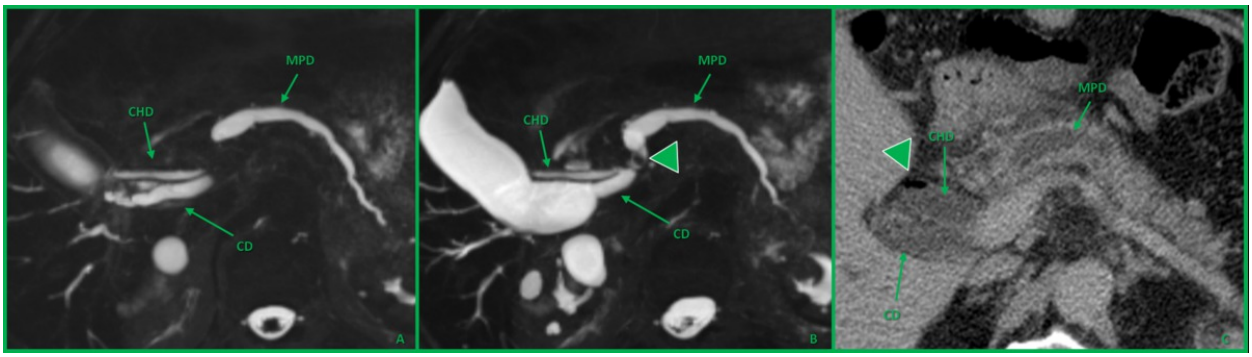

Fig. 17: "Parallel course between the cystic duct and the common hepatic duct". (A, B) Axial oblique MIP reformats demonstrate the parallel route between the cystic duct (CD) and the common hepatic duct (CHD). The CHD does not look fully distended because of the presence of intraductal air. The ductal dilation is caused by an ampullary stone (pointing triangle), which also causes dilation of the main pancreatic duct (MPD). (C) Axial non-contrast enhanced CT image clearly demonstrates an air-fluid level in the CHD (pointing triangle).

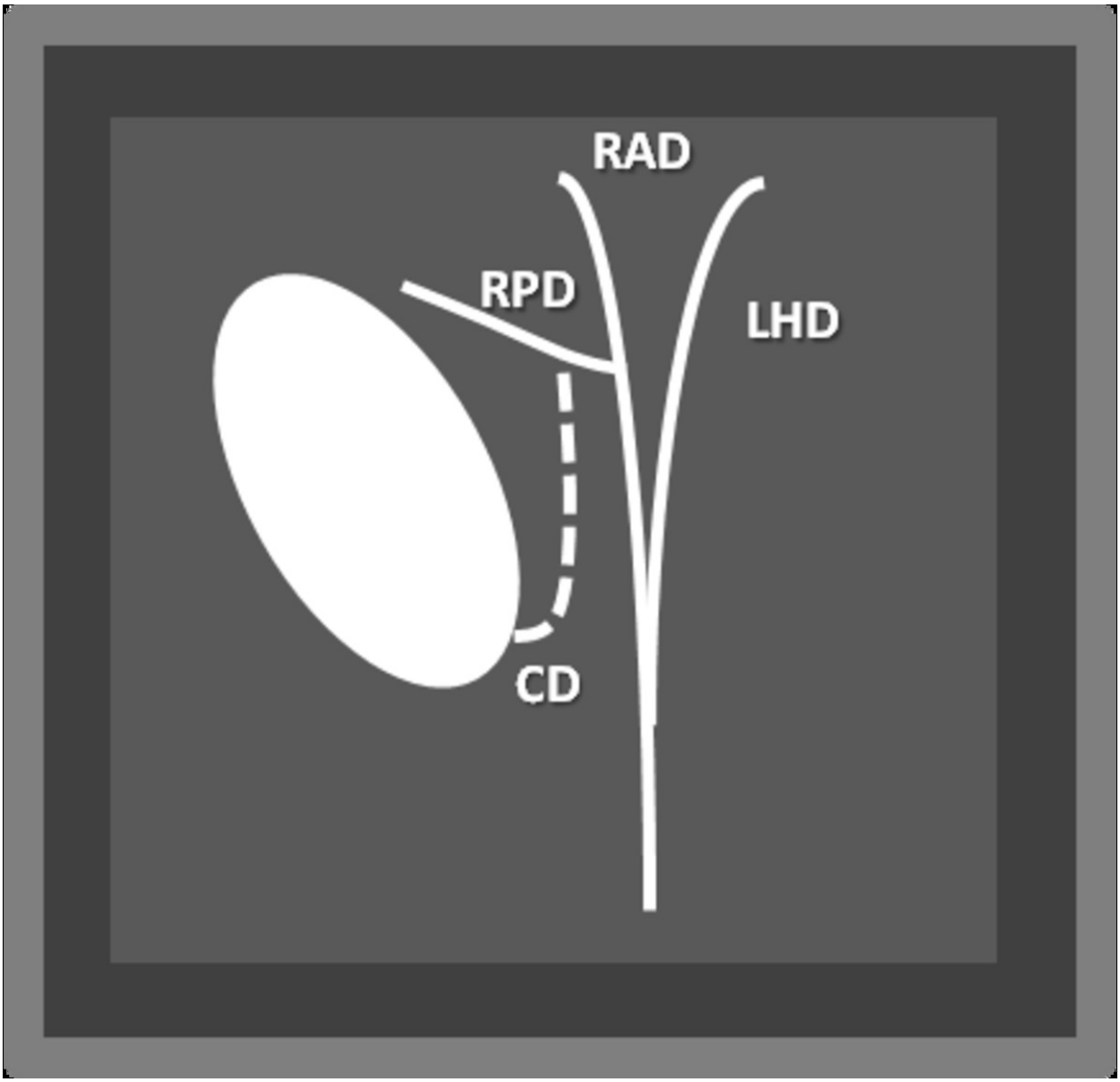

Fig. 18: "High insertion of the cystic duct in the right posterior duct". Schematic representation shows the insertion of the cystic duct (CD) in the right posterior duct (RPD). Right anterior duct (RAD), left hepatic duct (LHD).

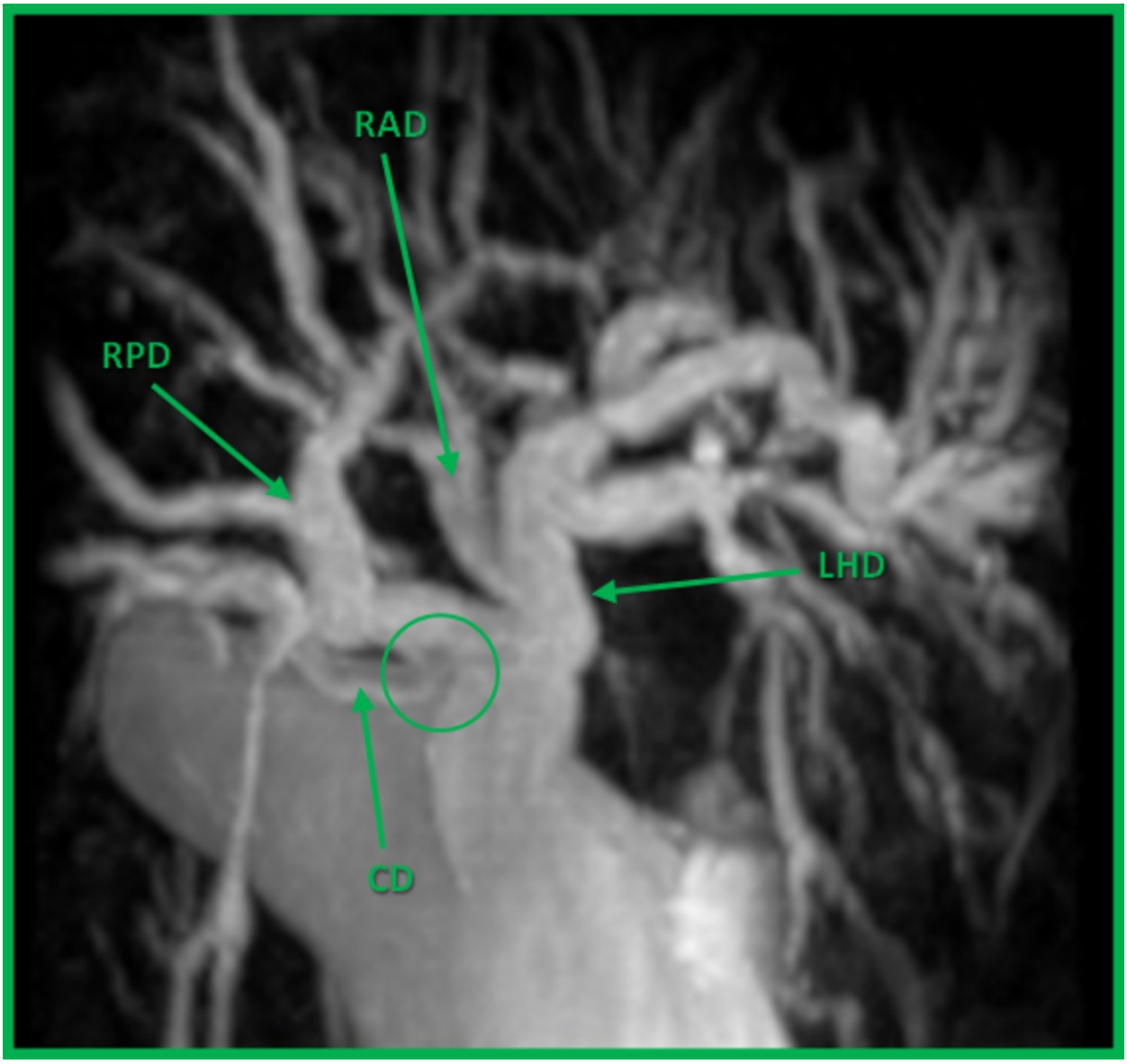

Fig. 19: "High insertion of the cystic duct in the right posterior duct". Coronal oblique MIP reformat shows the insertion of the cystic duct (CD) in the distal third of the right posterior duct (RPD). The confluence is marked by the circle. There is another anatomical variant, with the right anterior duct (RAD) joining the left hepatic duct (LHD).

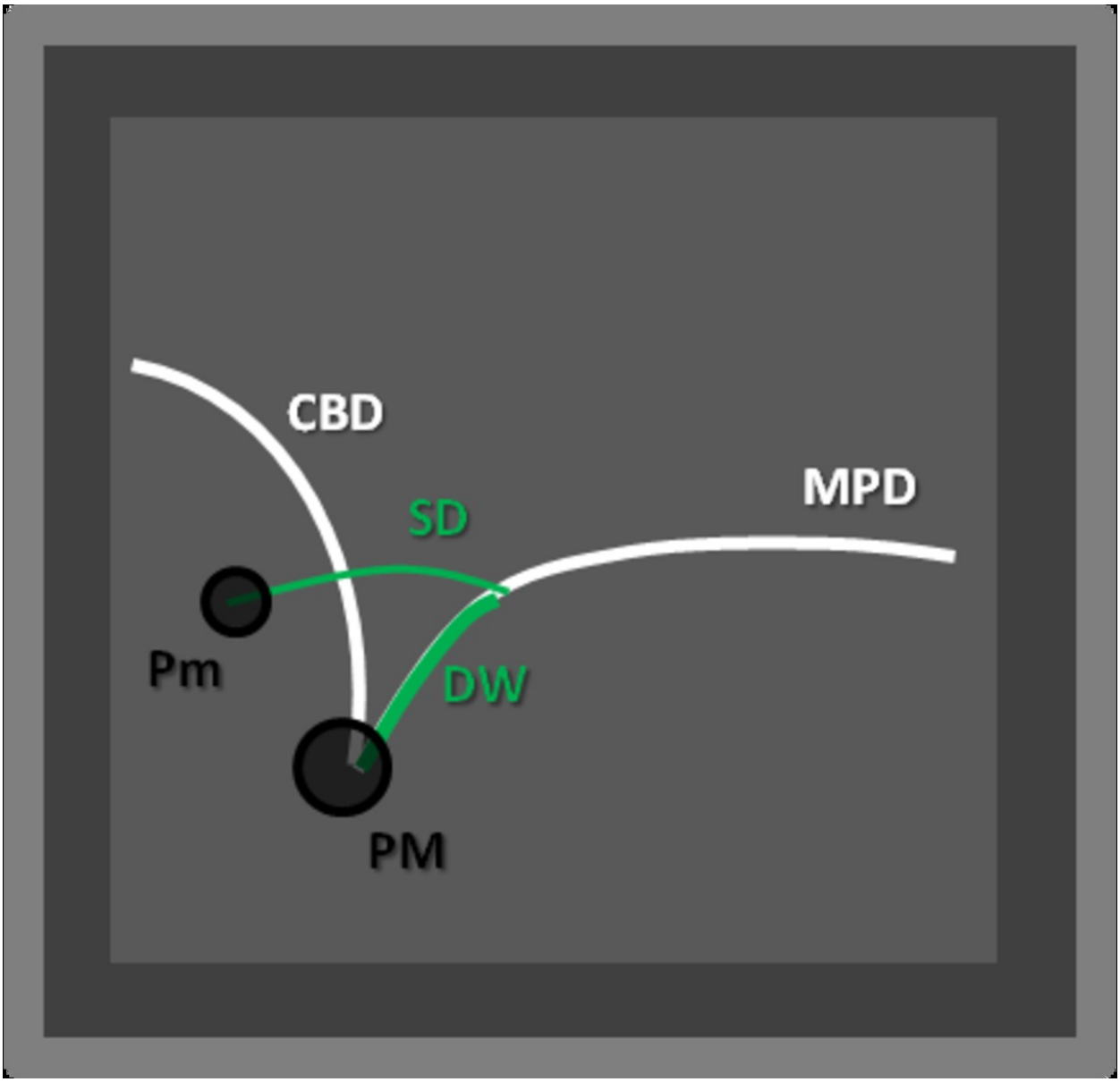

Fig. 20: "Normal pancreatic ductal anatomy". Schematic representation shows the main pancreatic duct (MPD) crossing the pancreas and continuing as the duct of Wirsung (DW) at the pancreatic head. At its distal portion the DW joins the common bile duct (CBD), draining into the major papilla (PM). The duct of Santorini (SD) drains into the minor papilla (Pm).

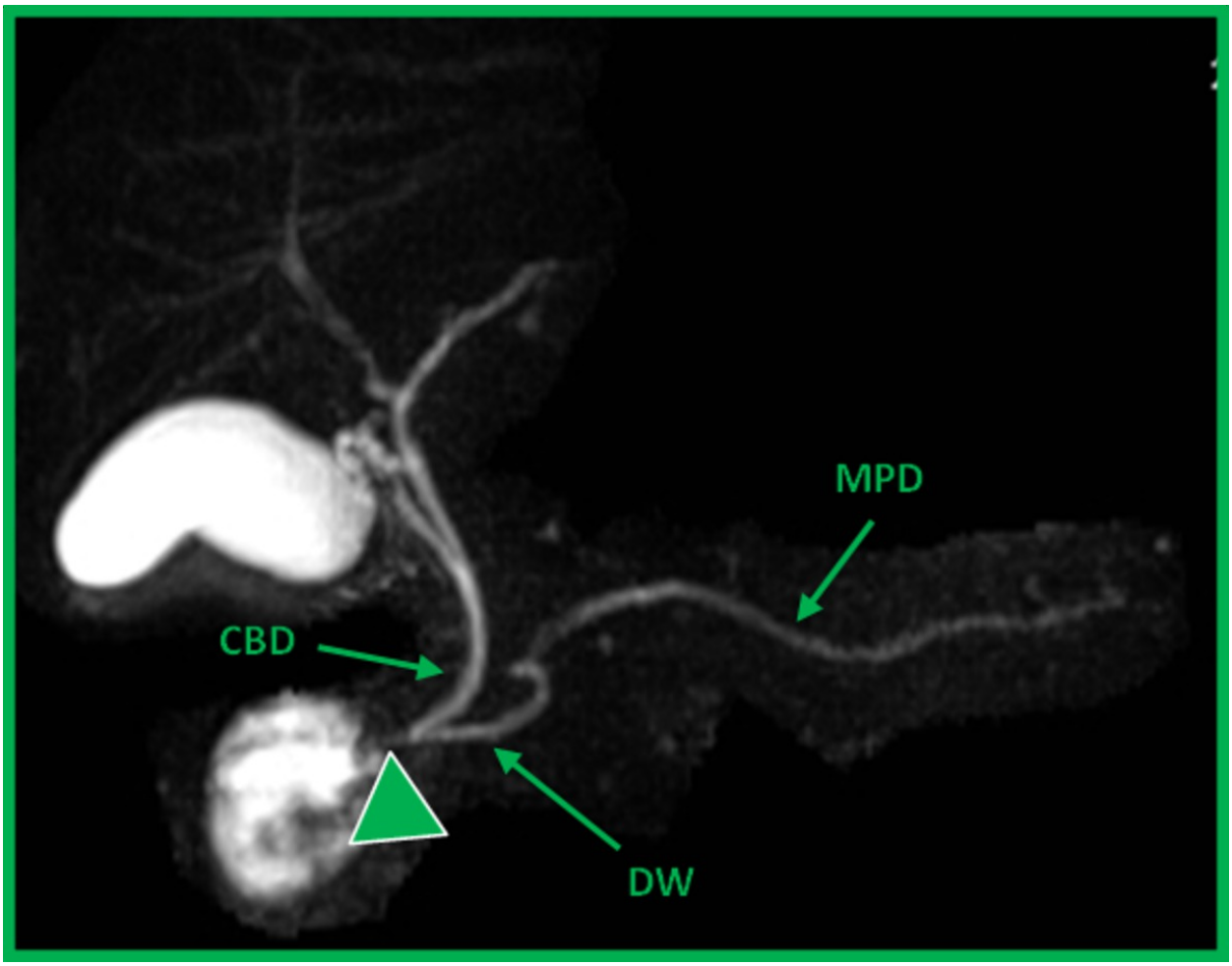

Fig. 21: "Normal pancreatic ductal anatomy". Coronal oblique reformat shows the main pancreatic duct (MPD) crossing the whole pancreas and continuing as the duct of Wirsung (DW) at the pancreatic head. At its distal portion the DW joins the common bile duct (CBD), draining into the major papilla (pointing triangle). The duct of Santorini is not demonstrated.

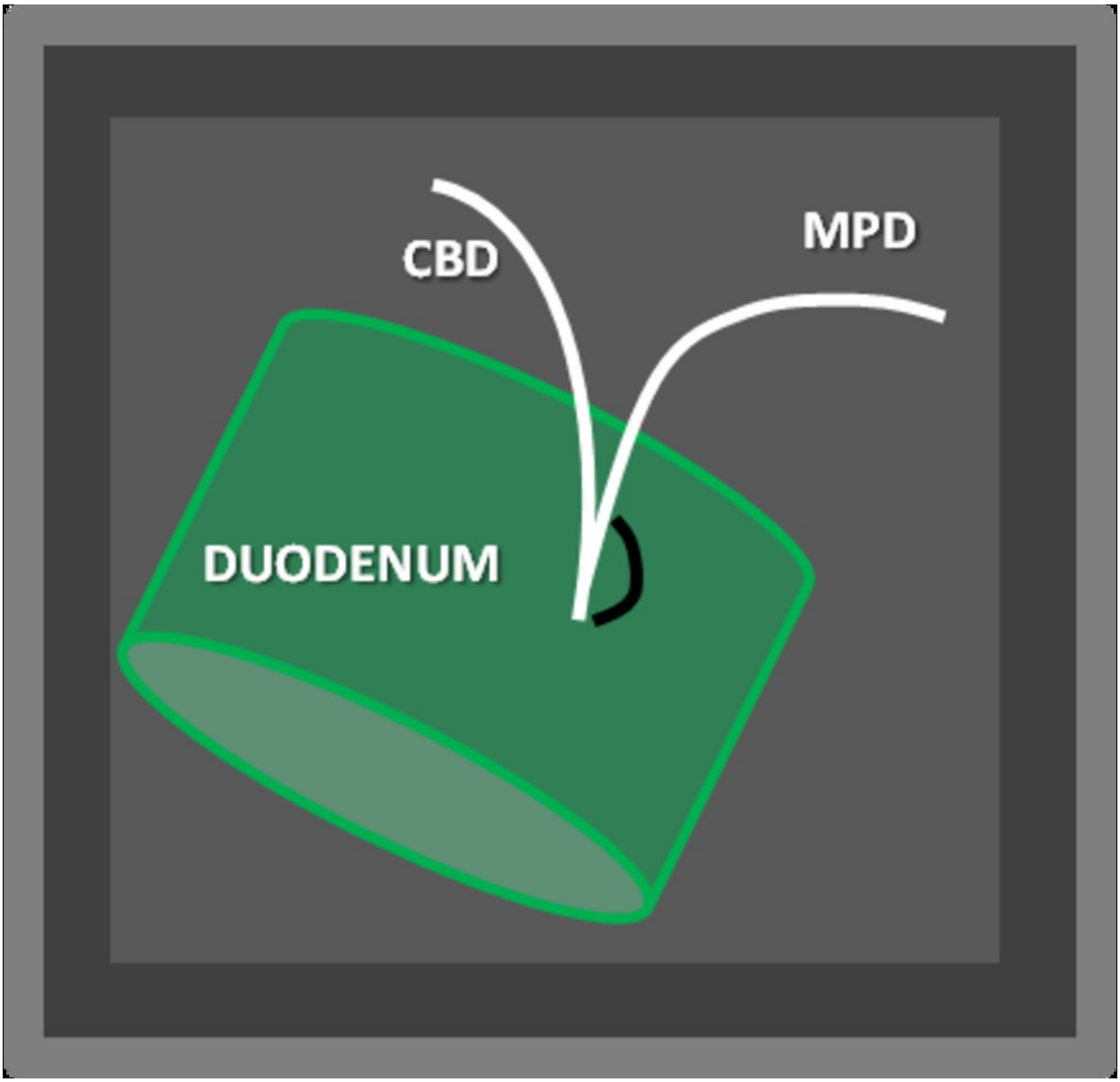

Fig. 22: "Pancreatobiliary junction". Schematic representation shows the normal intramural junction between the common bile duct (CBD) and the main pancreatic duct (MPD).

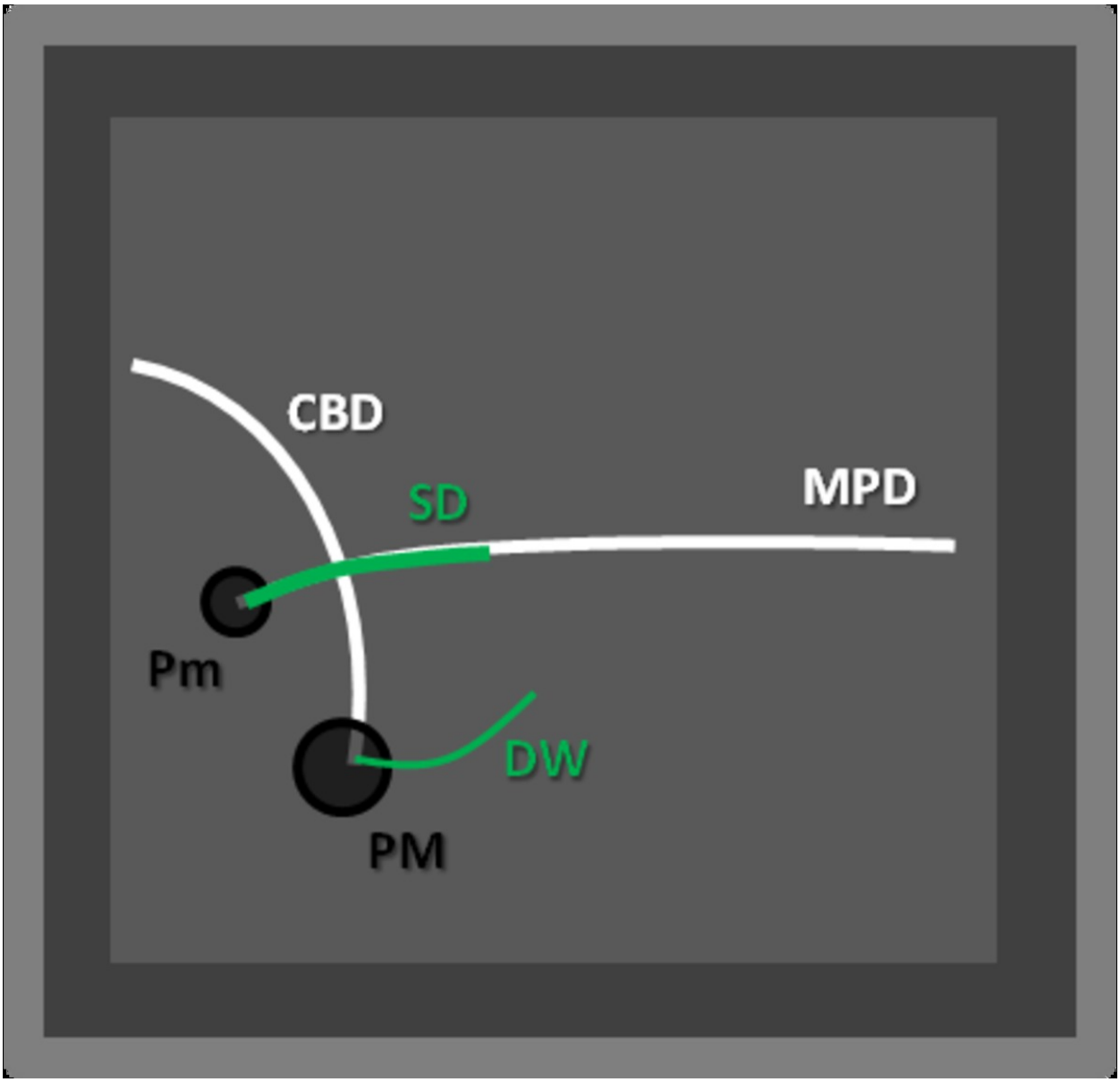

Fig. 23: "Complete pancreas divisum". Schematic representation demonstrates the main pancreatic duct (MPD) draining at the minor papilla (Pm) through the duct of Santorini (DS). The duct of Wirsung (DW) drains the ventral portion of the pancreas at the major papilla (MP), where it still joins the common bile duct (CBD). There is no communication between the DW and the DS.

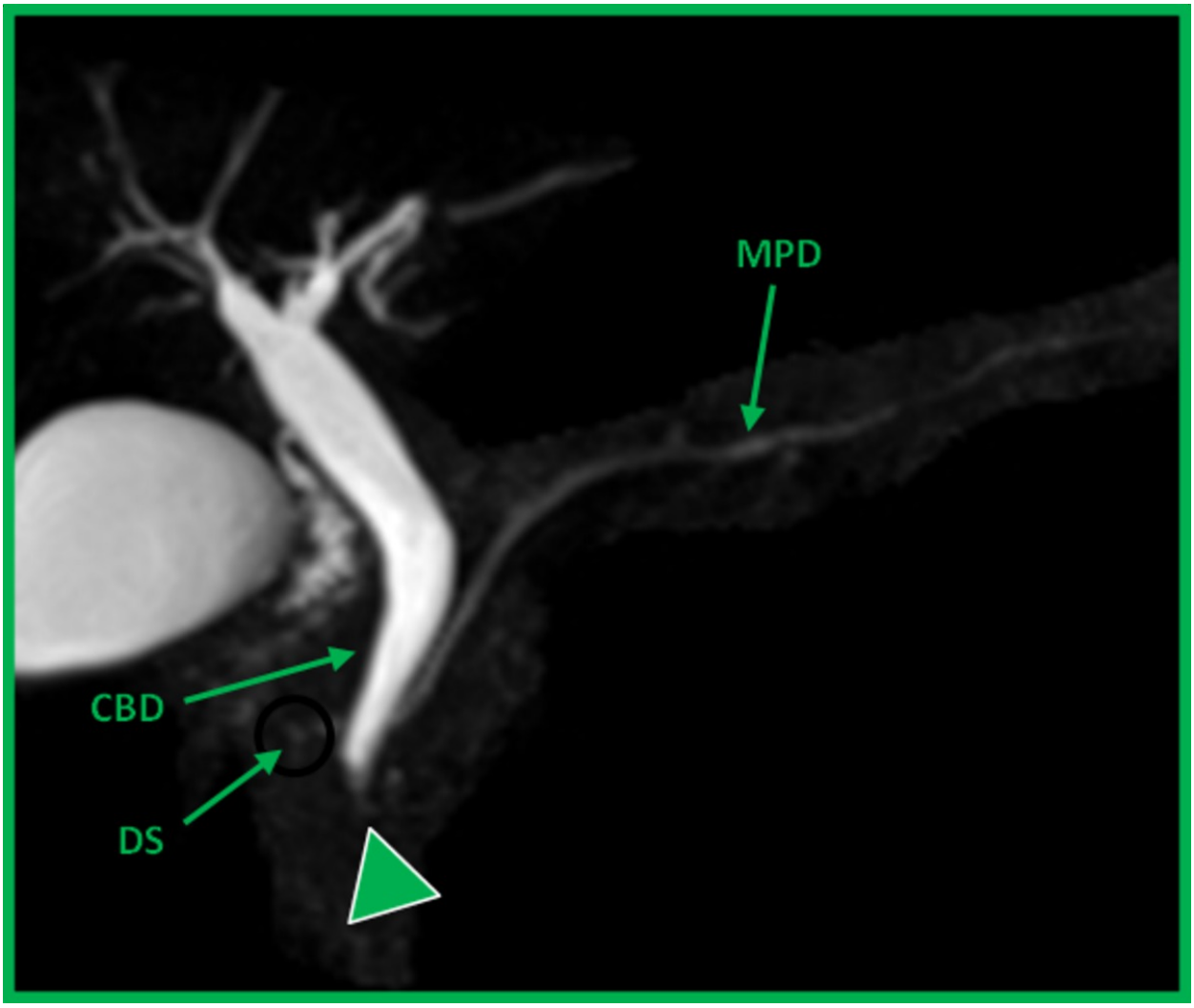

Fig. 24: "Complete pancreas divisum". Coronal oblique reformat shows the main pancreatic duct (MPD) draining at the minor papilla (black circle) through the duct of Santorini (DS), independently from the common bile duct (CBD) which drains at the major papilla (pointing triangle). There is no communication between the DS and the duct of Wirsung (the duct of Wirsung cannot actually be seen in the present image).

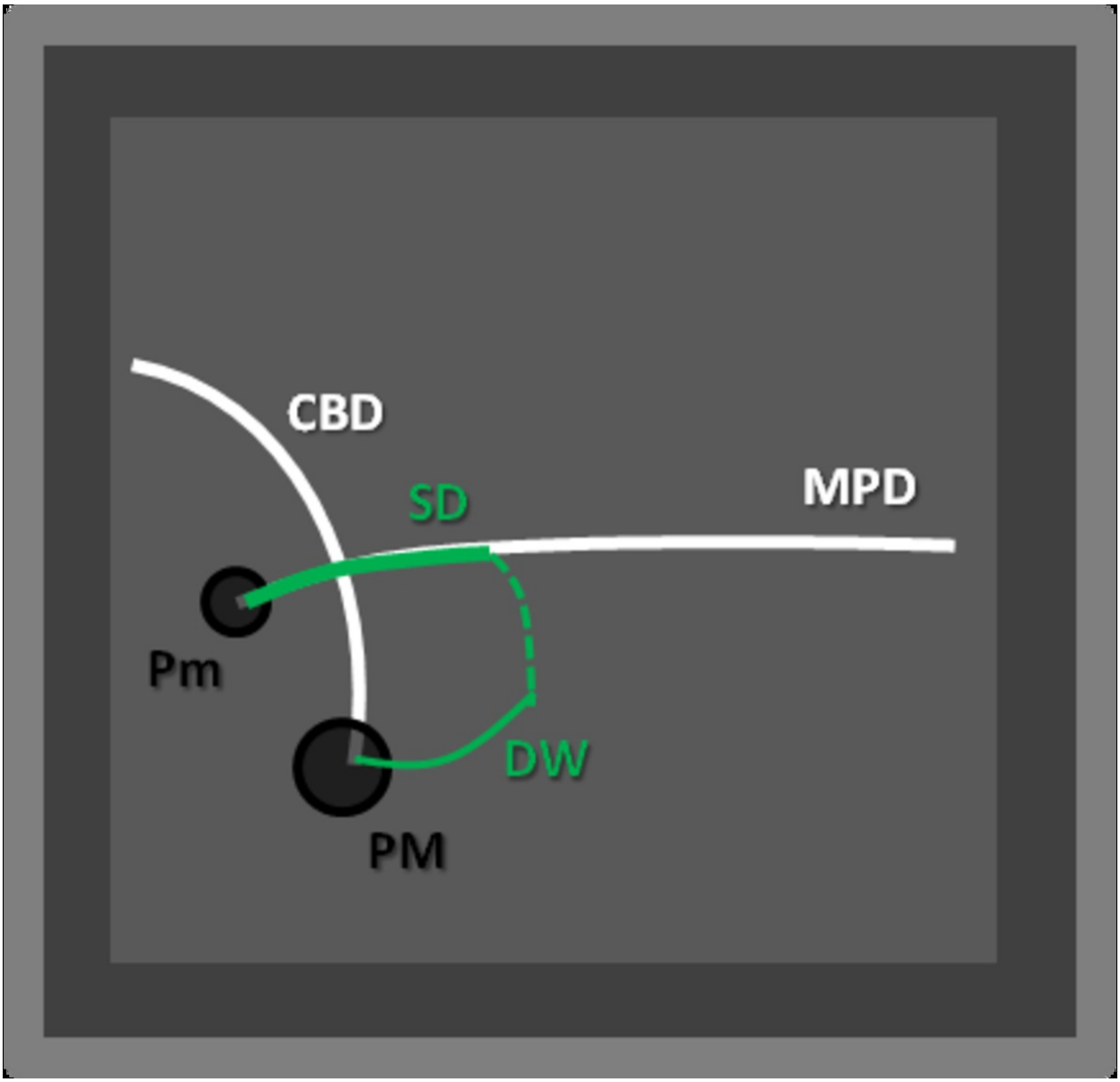

Fig. 25: "Incomplete pancreas divisum". Schematic representation demonstrates the main pancreatic duct (MPD) draining at the minor papilla (Pm) through the duct of Santorini (DS). The duct of Wirsung (DW) drains the ventral portion of the pancreas at the major papilla (MP), where it still joins the common bile duct (CBD). There is a communication between the DW and the DS.

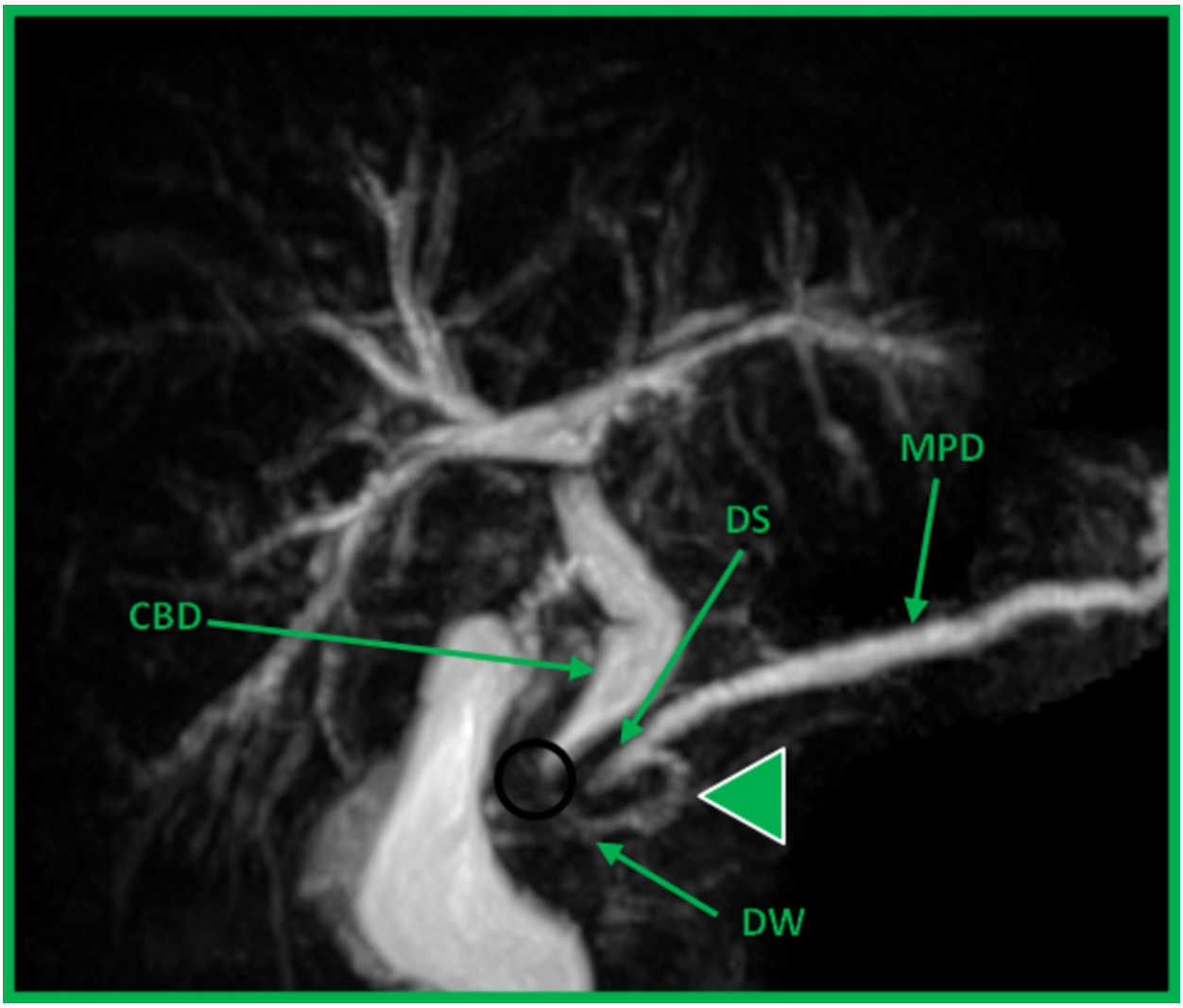

Fig. 26: "Incomplete pancreas divisum". Coronal oblique MIP reformat demonstrates the main pancreatic duct (MPD) draining at the minor papilla through the duct of Santorini (DS). The duct of Wirsung (DW) drains the ventral portion of the pancreas at the major papilla (black circle), where it still joins the common bile duct (CBD). There is a communication between the DW and the DS (pointing triangle).

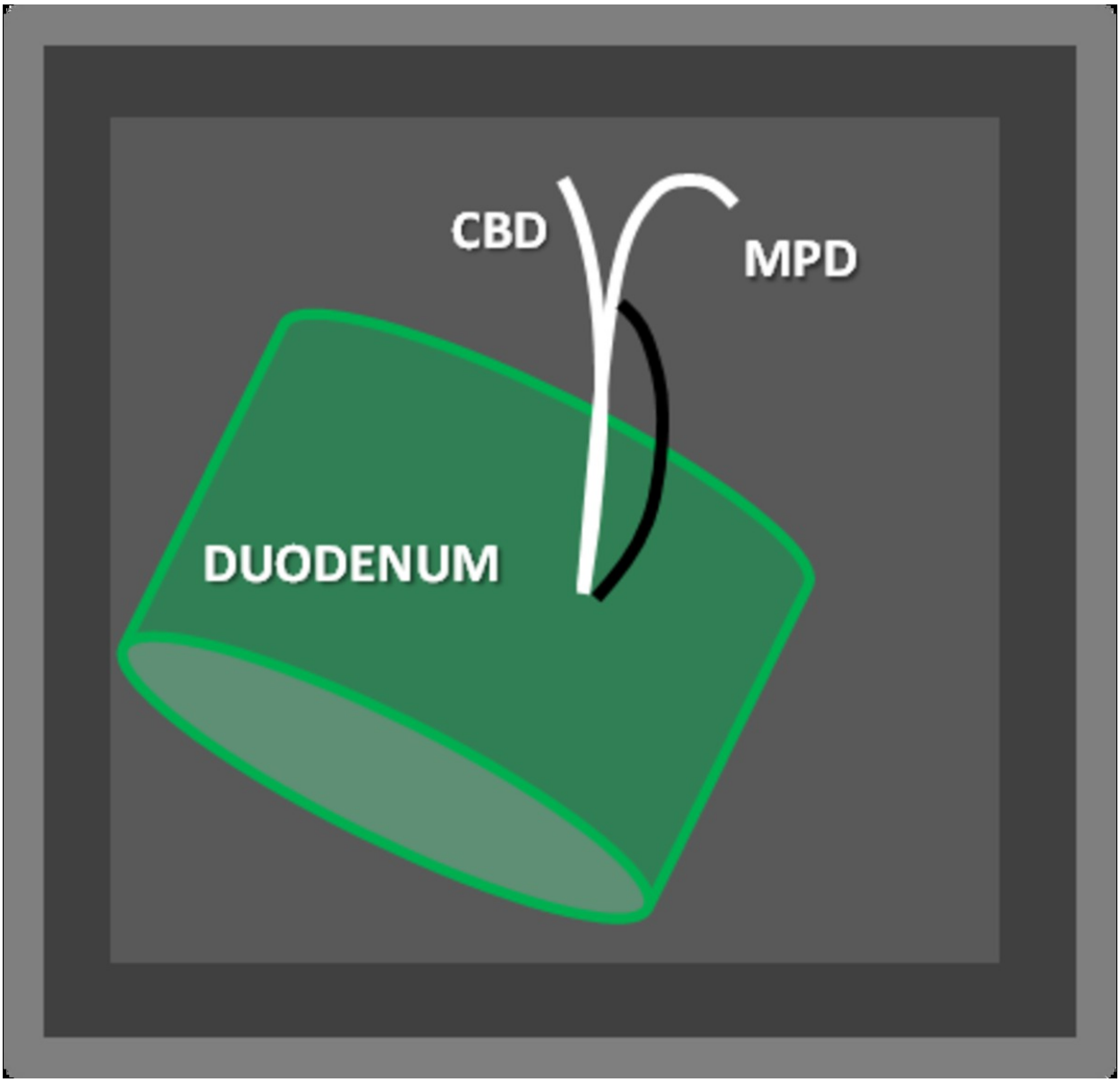

Fig. 27: "Anomalous pancreatobiliary junction". Schematic representation shows the abnormal junction between the common bile duct (CBD) and the main pancreatic duct (MPD) which occurs partially outside the duodenal wall.

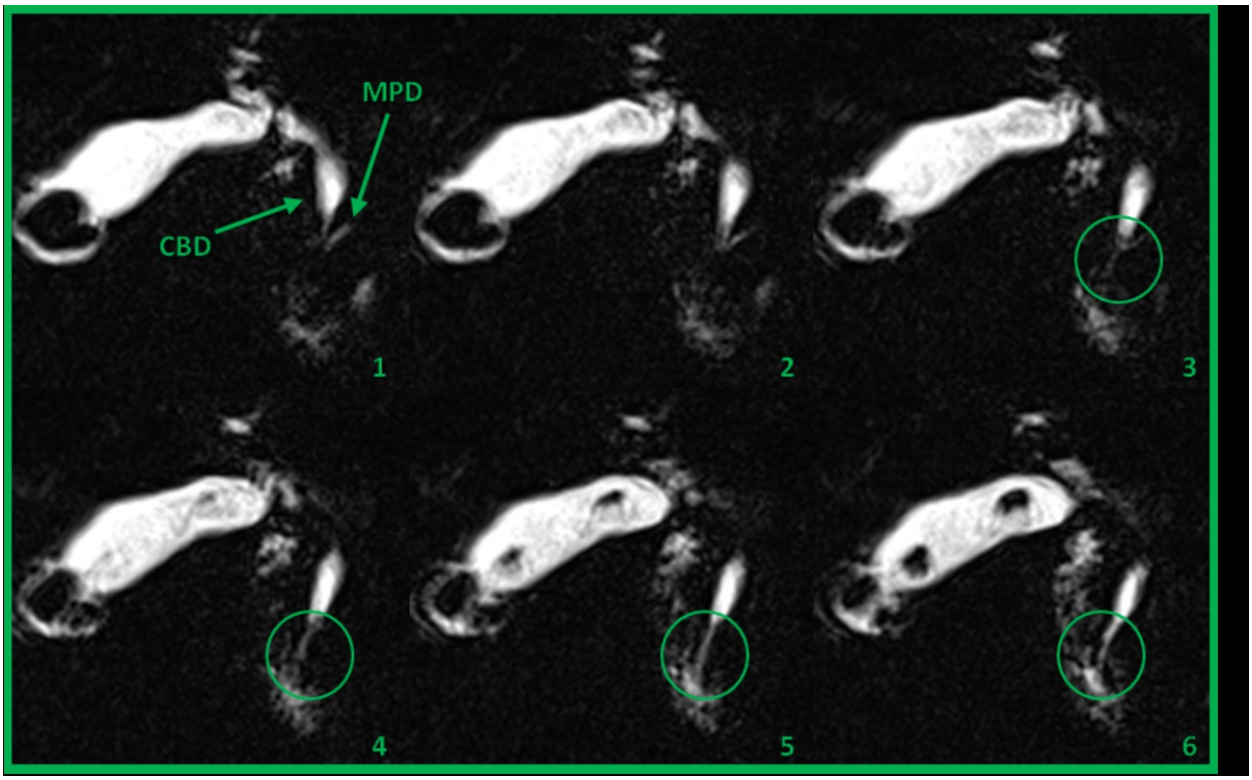

Fig. 28: "Anomalous pancreatobiliary junction". Sequence of six successive coronal oblique MIP reformat images reveal the abnormal junction between the common bile duct (CBD) and the main pancreatic duct (MPD), originating a long common channel (circle).

Conclusion

MRCP, a non-invasive technique, is an excellent diagnostic method to evalute pancreatobiliary tract, not only to investigate pathologies but also to delineate ductal anatomy, revealing possible anatomical variants. By this, familiarity with MRCP anatomical findings may help preventing iatrogenic complications.

Acknowledgments

The authors are most grateful to the MRI personnel of our department, particularly to the technicians David Monteiro and Nuno Almeida, for their important contribution to the accomplishment of this work.

Personal information

João Filipe de Azevedo Gomes de Carvalho Ressurreição

joaofres@gmail.com

References

1. Akisik MF *et al*. Dynamic Secretin-enhanced MR Cholangiopancreatography. Radiographics, May-June 2006; 26:3, 665-677
2. Borghei P *et al*. Anomalies, Anatomic Variants, and Sources of Diagnostic Pitfalls in Pancreatic Imaging. Radiology, January 2013; 266:1, 28-36
3. Gazelle GS, Lee MJ and Mueller PR. Cholangiographic Segmental Anatomy of the Liver. Radiographics, September 1994; 14:5 1005-1013
4. Griffin N, Charles-Edwards G and Grant LA. Magnetic Resonance Cholangiopancreatography: the ABC of MRCP. Insights Imaging, February 2012; 3:1, 11-21
5. Hyodo T *et al*. CT and MR Cholangiography: Advantages and Pitfalls in Perioperative Evaluation of Biliary Tree. Br J Radiol, July 2012; 85: 887-896
6. Mortelé KJ and Rós PR. Anatomic Variants of the Biliary Tree: MR Cholangiographic Findings and Clinical Applications. AJR, August 2001; 177: 389-394
7. Mortelé KJ *et al*. Multimodality Imaging of Pancreatic and Biliary Congenital Anomalies. Radiographics, May-June 2006; 26:3, 715-731.

8. Turner MA and Fulcher AS. The Cystic Duct: Normal Anatomy and Disease Processes. Radiographics, January 2001; 21:1, 3-22.
9. Yu J *et al*. Congenital Anomalies and Normal Variants of the Pancreaticobiliary Tract and the Pancreas in Adults: Part 1, Biliary Tract. AJR, December 2006.; 187:6, 1536-1543
10. Yu J *et al*. Congenital Anomalies and Normal Variants of the Pancreaticobiliary Tract and the Pancreas in Adults: Part 2, Pancreatic Duct and Pancreas. AJR, December 2006.; 187:6, 1544-1553